# CHARACTERIZATION OF ENDOPLASMIC RETICULUM TARGETING LIPOSOMES AS DRUG DELIVERY VESICLES

**Kelly Masterson Skelton**

**Hertford College, Oxford**

MASTER OF SCIENCE BY RESEARCH

DEPARTMENT OF BIOCHEMISTRY

UNIVERSITY OF OXFORD

2012

# Acknowledgements

I would like to thank Professor Nicole Zitzmann for her guidance and support and giving me the opportunity to complete this research and for being an inspiration. I am very grateful to Professor Raymond Dwek for his encouragement and motivation; it is a privilege. Thanks to Drs. Stephanie Pollock and Sally Latham for their scientific advice and expertise and teaching me new technical skills that enabled this research. Thank you to Baruch Blumberg and his family, Raymond Dwek, and The Glycobiology Institute for financial assistance through the Baruch Blumberg Scholarship. Thank you to Dr. Terry Butters and Dr. Paul Wentworth for letting me use their analytical instruments, HPLC-PAD and HPLC-UV, respectively. Thank you to United Therapeutics Inc for providing the iminosugar compounds. Thanks to the Dunn School for use of their confocal microscopes. Thank you to my husband, Peter, and to my family for their steadfast support. Special thanks to my departed grandfather, Donald Pontius, who inspired me with scientific challenges as a young child, taught me to work hard, and to believe in myself.

"The intellect hates vacuums," Baruch Blumberg, *Hepatitis B, The hunt for a killer virus*.

# Abstract

Due to rapid viral and drug resistance mutations, there is a great need for broad-spectrum antiviral therapies that target the host rather than viral processes. This research builds upon previous studies developing α-glucosidase inhibitors known as iminosugars as broad-spectrum antiviral drugs. Initially pH-sensitive liposomes were designed and developed as drug delivery vehicles to enhance cellular internalization for α-glucosidase inhibitors for HIV-1 antiviral treatment. Recent studies by Pollock *et al.* have shown that polyunsaturated endoplasmic reticulum targeting liposomes known as PERLs, traffic to the ER and are antiviral as a stand-alone therapy against hepatitis B, hepatitis C, and HIV. In addition, α-glucosidase inhibitors formulated and delivered by 'ER-targeting' liposomes have shown potential in recent preclinical studies *in vitro* and are candidates for future clinical trials as antiviral treatments.

There are two main purposes of this research. Firstly, it aims to develop crucial quantitative analytical methods that detect the α-glucosidase inhibitor drugs when formulated in 'ER-targeting' liposomes. The analytical methods will help elucidate how the chemical properties of small molecules, such as hydrophobicity or polarity, affect the encapsulation efficiency into 'ER-targeting' liposomes, which will help select appropriate formulation processes and dosing regimes for potential future clinical trials. Secondly, this research intends to dissect the possible cellular internalization and trafficking pathways that the 'ER-targeting' liposomes, such as PERLs, utilize to get to the ER *in vitro*. A large screening assay was conducted to determine what influence each type of

phospholipid has on the cellular entry and intracellular movement of ‘ER-targeting’ liposomes. Several key observations were drawn from this research that will hopefully further the knowledge of ‘ER-targeting’ liposomes’ capability to deliver iminosugars and the pathways involved with the cellular internalization and trafficking of the liposomes *in vitro*.

# Table of Contents

**Acknowledgements** **2**

**Abstract** **3**

**Table of Contents** **5**

**List of tables** **8**

**List of figures** **10**

**Chapter One: Introduction** **12**

Research aims 19

**Chapter two: Methodology** **20**

2.1 Formulation of liposomes using the reverse phase evaporation method 20

2.2 Separation of liposomes from free calcein/un-encapsulated drug 21

2.3 Compound extraction from liposomes and solid phase extraction to remove lipids from the sample matrix 22

2.3.1 Compound extractions 22

2.3.2 Solid phase extraction of lipids from sample matrix 22

2.4 Calcein encapsulation determination 23

2.5 Cell culture 23

2.6 MTS cell toxicity assay 24

2.7 Liposome uptake assays 24

2.8 Dynamic light scattering (DLS) analysis of liposomes 25

**Chapter three: Determination of encapsulation efficiency of iminosugars in endoplasmic reticulum (ER) targeting liposomes** **26**

3.1 Introduction 26

3.2 Experimental design 31

3.3 Methodology optimized for the determination of the encapsulation efficiencies of iminosugars in liposomes 33

3.4 Results 39

3.4.1 Calcein encapsulation efficiency 39

3.4.2 *N*B-DNJ extraction from liposome sample matrix 39

3.4.3 *N*B-DNJ quantitative analysis 40

3.4.4 Encapsulation of *N*B-DNJ in liposomes 42

3.4.5 NAP-DNJ quantitative analysis 45

3.4.4 Encapsulation of NAP-DNJ in liposomes 47

**Chapter four: Cellular uptake and trafficking of endoplasmic reticulum (ER) targeting liposomes** **52**

4.1 Introduction 52

4.2 Experimental design 59

4.3 Results 65

4.4 Discussion 75

**Chapter five: Conclusions** **79**

**Appendices** **87**

Appendix A: Chemical structures 87

Appendix B: Materials 91

Appendix C: Protocols 94

Protocol for preparing liposomes using reverse phase hydration 94

**References** **97**

# List of tables

Table 1: Results of study to determine the optimal extraction buffer to be used to extract *N*B-DNJ from PERLs, N = 3. 39

Table 3: Comparing the linearity of the encapsulation efficiency of *N*B-DNJ in 5 mM pH-sensitive liposomes and in 5 mM PERLs determined by the RP-RID method 3. N=6 43

Table 5: Results of study to determine the optimal extraction buffer to be used to extract *N*B-DNJ from PERLs analyzed by RP-UV HPLC method 4, N=3. 46

Table 7: 16 inhibitors of endocytosis and intracellular trafficking mechanisms used in this study to identify the cellular endocytosis and trafficking pathways affected by liposomes with various concentrations of phospholipids (2 pages). 55

Table 5: Experimental design for cellular uptake and trafficking of endoplasmic reticulum (ER) targeting liposomes study- 25 formulations with unique phospholipid compositions. The final volume the lipids were suspended in resulted in the final formulation concentration of 5 mM. (See Appendix A1 and the list of abbreviations for clarification). 60

Table 10: Liposomal formulation concentrations for MTS cellular toxicity assay. 61

Table 12: The range of optimal cellular endocytosis and trafficking inhibitor concentrations and incubations times to be used for the MTS assay to determine the cellular toxicity in Huh7.5 cells. 62

Table 14: Example of 96-well plate design for rhodamine labeled liposome uptake in Huh7.5 cells in the presence of cellular endocytosis and trafficking inhibitors (one

concentration). One 96-well plate per formulation per inhibitor concentration. See Table 7 for abbreviations. 64

Table 16: Highest concentration of each liposome formulation incubated with Huh7.5 cells for 1 hour while maintaining <5% cellular toxicity determined by an MTS assay. 68

Table 10: Highest concentration of each endocytosis inhibitor incubated for 30 minutes with Huh7.5 cells while maintaining <5% cellular toxicity determined by an MTS assay. 68

Table 19: Mean percent uptake of rhodamine labeled liposome formulations in the presence of clathrin and caveolae endocytosis inhibitors. Key Red >110%, 70% < white > 110%, 30% < light green > 70%, dark green < 30% uptake. 70

Table 12: Mean percent uptake of rhodamine labeled liposome formulations in the presence of cholesterol depletion, dynamin I & II, and actin polymerization inhibitors. Key: Red >110%, 70% < white > 110%, 30% < light green > 70%, dark green < 30% uptake. 71

Table 13: Mean percent uptake of rhodamine labeled liposome formulations in the presence of endosomal acidification and microtubule inhibitors. Key: Red >110%, 70% < white > 110%, 30% < light green > 70%, dark green < 30% uptake. 72

Table 23: Mean percent uptake of rhodamine labeled liposome formulations in the presence of micropinocytosis inhibitors. Key: Red >110%, 70% < white > 110%, 30% < light green > 70%, dark green < 30% uptake. 73

Table 15: Summary of the cellular internalisation and trafficking mechanisms utilized by liposomes of varying phospholipid composition. 74

# List of figures

Figure 1: Overview of the effects of *N*-alkylated DNJ inhibition of carbohydrate processing (Mellor *et al.*, 2004). 13

Figure 3: pH-sensitive liposome intracellular trafficking along the endosomal pathway destabilizes the liposome lipid bilayer as the pH decreases (adapted from Pollock, 2008b).15

Figure 5: Diagram illustrating the main modes of endocytosis and intracellular transport mechanisms (Soldati & Schliwa, 2006). 17

Figure 6: Diagram of the pulse sequence to detect carbohydrates using PAD (Dionex Corporation, 2000). 29

Figure 8: Experimental overview for determining the encapsulation efficiency of iminosugars in ER-targeting liposomes. 32

Figure 9: HPLC-RID chromatogram of *N*B-DNJ using the RP-RID method 3. 41

Figure 11: HPLC-RID chromatogram showing analysis of 50 mM *N*B-DNJ in 5 mM PERLs using RP-RID method 3. 41

Figure 13: Comparing the encapsulation efficiency of *N*B-DNJ in 5 mM pH-sensitive liposomes (blue) and PERLs (green), n=6. 44

Figure 15: HPLC-UV chromatogram of 1 mM NAP-DNJ analyzed by RP-UV method 4. 45

Figure 17: Sample chromatogram of 1 mM NAP-DNJ in 5 mM PERLs formulation analyzed by the gradient RP-UV detection method 5. 46

Figure 19: The encapsulation efficiencies of NAP-DNJ in PERLs analyzed by the RP-UV method 5, N = 3 (Tang, 2012). 47

Figure 21: Colocalization of Rh-PE-labeled liposomes with ER marker, EDEM, in Huh7.5 cells using confocal microscopy (Pollock, 2010a). 53

Figure 23: Inhibitors of endocytosis and intracellular trafficking mechanisms (adapted from Pollock, 2008). 54

Figure 25: Uptake of 1% rhodamine PE labeled liposomes in the presence of inhibitors of endocytosis and vesicle trafficking in Huh7.5 cells (Pollock *et al.*, 2010a). 57

Figure 27: Analysis of liposomal formulations, 1 and 19, by dynamic light scattering (DLS) analysis. 66

Figure 29: Comparison of uptake of rhodamine labeled monounsaturated ‘ER-targeting’ liposome data from this experiment to the data observed for the previously published data (Pollock *et al*., 2010a). 74

# Chapter One: Introduction

Over the last forty years, α-glucosidase inhibitors, specifically iminosugars, have been developed, modified, and proven to be effective against a wide range of viruses and diseases (Paulsen & Brockhausen, 2001). Iminosugars are sugars in which the endocyclic oxygen is replaced by a basic nitrogen atom. The first recorded synthesis of 1-deoxynojirimycin DNJ was in 1966 by Paulsen and later found naturally in mulberry leaves (Compain *et al*., 2006). Later *N*-butyl-deoxynojirimycin (*N*B-DNJ) also known as Miglustat and marketed under the name Zavesca, a glucosylceramide synthase inhibitor, became a treatment for type I Gaucher's disease and Niemann-Pick type C disease (Elstein *et al.*, 2004). More recently, *N*-alkylated iminosugars have been designed, synthesized, and shown to allow a more selective approach for molecular inhibition of both ceramide glucosyltransferase and α-glucosidase I allowing them to be effective drugs against lysosomal storage disorders and viral infections, respectively (Chapel *et al.*, 2007; Fischer *et al.* 1996; Mellor *et al*., 2000, 2004). Figure 1 shows the mechanism of action for *N*-alkylated iminosugar inhibition on carbohydrate processing.

**Figure 1: Overview of the effects of *N*-alkylated DNJ inhibition of carbohydrate processing (Mellor *et al.*, 2004).**

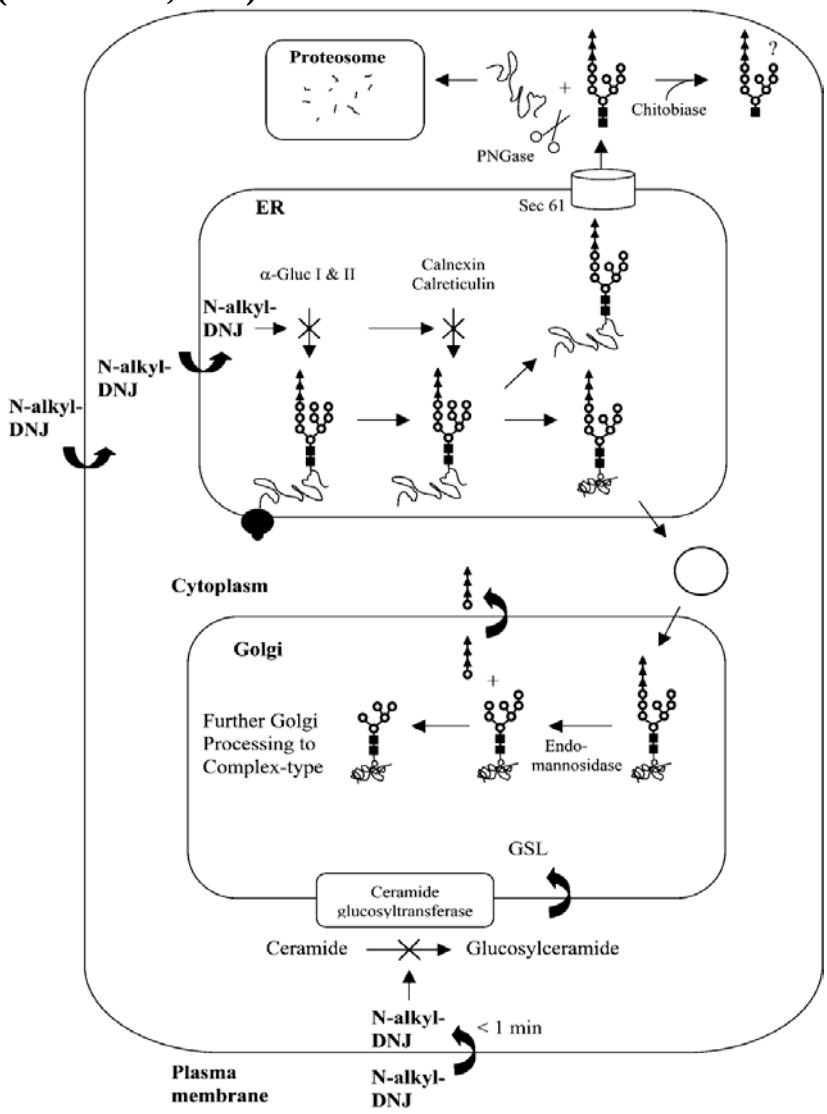


*N*-alkylated DNJ analogues rapidly enter the cell (<1 min). The *N*-butyl/N-nonyl derivatives gain access to the lumen of the ER and inhibit N-linked oligosaccharide trimming by a-glucosidases I and II. For glycoproteins that require calnexin/calreticulin for correct folding, retention of two or three glucose residues prevents the interaction of the glycoprotein with the chaperone(s). The misfolded protein may still be processed to the final destination or may be translocated to the cytosol via the Sec61 channel. The sites of action of *N*-alkylated DNJs are shown, together with the relative rates of intracellular access. No information regarding the rate of ER entry is available. *N*-Alkyl-DNJ compounds also inhibit CGT that synthesizes glucosylceramide, the precursor for most GSLs (Mellor *et al.*, 2004).

*N*B-DNJ has been shown to be an effective treatment against many human viruses *in vitro*, including hepatitis C (HCV), hepatitis B (HBV), human immunodeficiency virus (HIV), West Nile, dengue, and parainfluenza (Block *et al.*, 1994; Chapel *et al.*, 2007; Fischer *et al.*, 1995; Jordan *et al.*, 1992; Tanaka *et al*., 2006; Wu *et al.*, 2002). *N*B-DNJ has been shown to inhibit HIV-1 infectivity by 80% and HIV-2 infectivity by 95% at $IC_{50}$ concentrations of 282 μmol/l and 211 μmol/l, respectively (Pollock *et al.*, 2008a). *N*B-DNJ is known to react with the sucrase isomaltose enzyme of the intestinal lumen *in vivo* at these concentrations (Brennan *et al.*, 1995; Fischl *et al.*, 1994; Ratner *et al.*, 1993; Tierney *et al.* 1994). Due to this side effect, alternative delivery methods were examined in order to minimize the concentrations needed to decrease viral titers. Initially, pH-sensitive liposomes containing a 3:2 ratio of phosphotidylethanolamine (PE): cholesterol hemisuccinate (CHEMS) were used as the drug delivery vehicle for *N*B-DNJ treatment against HIV, providing a 100,000 enhancement in $IC_{50}$ values (Pollock *et al.*, 2008a). Endocytosis appears to be cell-line dependent and still remains a controversial point (Doherty & McMahon, 2009). Encapsulated compounds are transported into the cytoplasm through destabilization of or fusion with the endosome membrane (Simoes *et al.*, 2001). pH-sensitive liposomes are acidified as shown in Figure 2 as they move from early to late endosomes and finally in the lysosomes. The encapsulated cargo is released due to the protonation and destabilization of the lipid bilayer of the pH-sensitive liposomes in the late endosomal stage.

**Figure 2: pH-sensitive liposome intracellular trafficking along the endosomal pathway destabilizes the liposome lipid bilayer as the pH decreases (adapted from Pollock, 2008b).**

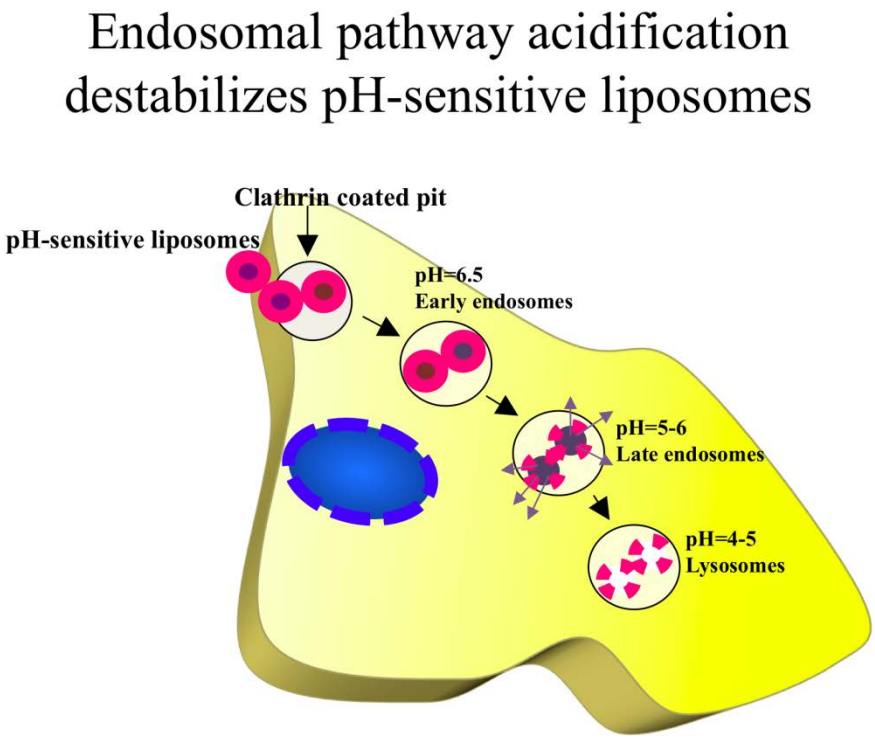


pH-sensitive liposomes move intracellularly through the endosomal pathway. The lipid bilayar (red) destabilizes as the pH decreases as they endosomal pathway acidifies. The contents of the lumen of the liposome are released at the late endosomes when the lipid bilayer destabilizes. The liposomes degrade in the acidic lysosome.

Although pH-sensitive liposomes aid cargo in crossing the plasma membrane, polyunsaturated endoplasmic reticulum targeting liposomes (PERLs) were developed by Pollock *et al.* to target specifically the ER, the site of protein translation and ER-budding viruses, such as HCV and bovine diarrhea virus (BVDV). Original PERL formulations were designed to resemble the ER-membrane composition that comprises of 57% phosphatidylcholine (PC), 24% PE, 13% phosphatidylinositol (PI), 3% phosphatidylserine (PS), and 3% sphingomyelin (SM) (Swift, 1995). The PERL formulations achieved 88% colocalization with the ER marker, EDEM (ER degradation-enhancing α-mannosidase like protein), while pH-sensitive liposomes only colocalized 13% (Pollock *et al.*, 2010a). A final ratio of 1.5:1.5:1:1 PC:PE:PI:PS was used for ease of formulation preparation since the percent of colocalization with EDEM, was comparable to the 57% PC, 24% PE, 13% PI, 3% PS formulation that resembled the ER membrane phospholipid composition (Pollock, 2008b). The PERLs were antiviral against HIV-1 and HCV (Pollock *et al.*, 2010b).

'ER-targeting' lipsosomes with a diameter of 100-200 nm potentially have the option of using clathrin-mediated endocytosis, caveolae-mediated endocytosis, phagocytosis, macropinocytosis, and non-clathrin-non-caveolae-dependent endocytosis as cellular internalisation mechanisms (Huth, 2006), or a combination thereof. These modes of cellular internalisation and movement are illustrated in Figure 3.

**Figure 3: Diagram illustrating the main modes of endocytosis and intracellular transport mechanisms (Soldati & Schliwa, 2006).**

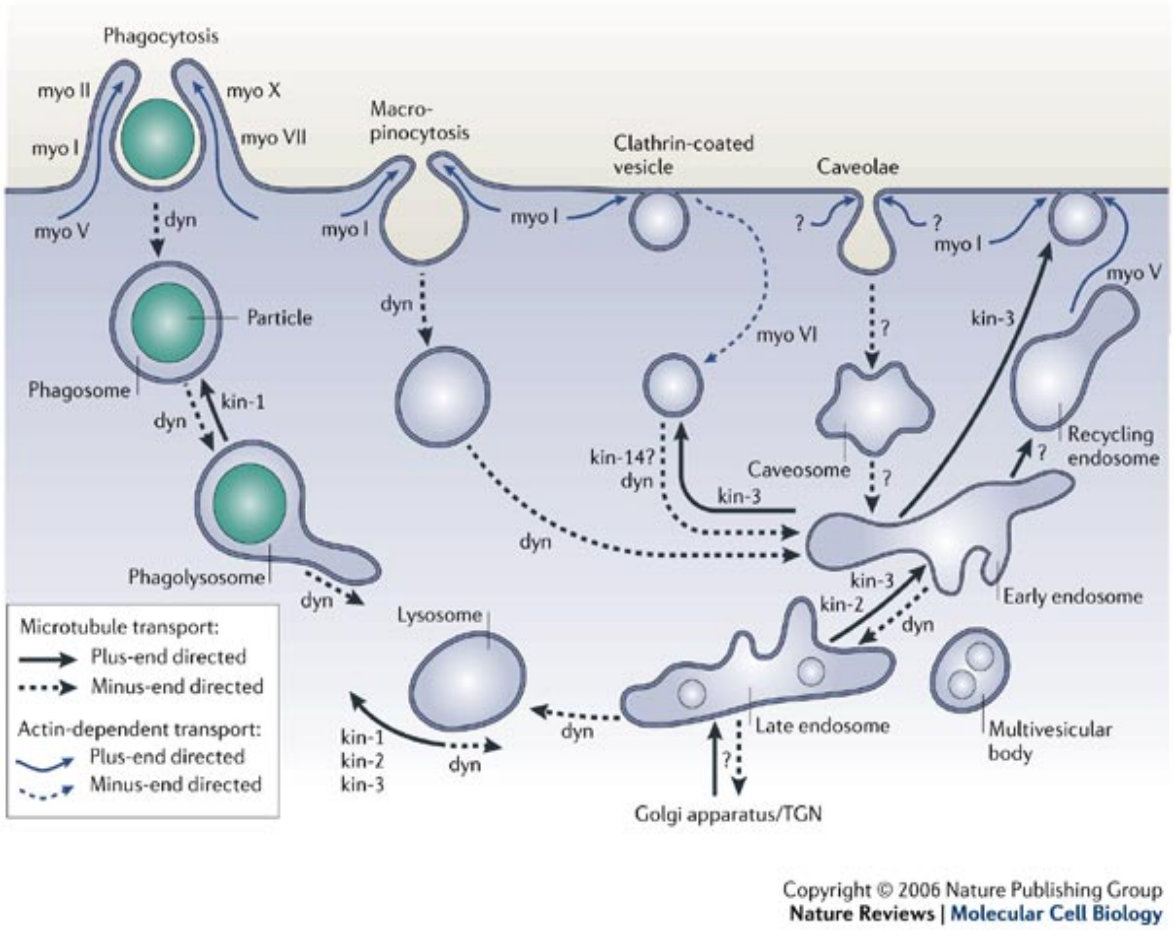

**Figure 3:**
The figure is compiled from studies that used a wide range of organisms, from amoebae to mammals. Endocytic cargoes are transported around cells along actin filaments or microtubules. The different classes of myosin (myo), kinesin (kin) or dynein (dyn) that have been implicated at each step are shown. In the three pinocytic pathways, macropinocytosis, the clathrin-dependent pathway and the caveolae pathway, internalized vesicles are transported to the early sorting station (early endosome). In the caveolar pathway, a compartment before the early endosome compartment, the caveosome, has been identified. Cargoes travel from early to late endosomes via endosomal carrier vesicles, also called multivesicular bodies, because they usually acquire internal membrane profiles as a result of the inward invagination of the restricted membrane. The cargoes that are destined for degradation then continue their journey to lysosomes, whereas others are recycled either to the plasma membrane (directly or through recycling endosomes) or to the Golgi apparatus (specifically to the trans-Golgi network (TGN)). Subsequently, these cargoes, together with newly synthesized proteins, can exit the TGN and traffic either to the plasma membrane or to late endosomes, and to a minor extent to early endosomes (not shown). Solid particles are taken up by phagocytosis into phagosomes, which are similar to the early endosome compartments of the pinocytic pathway. Phagosomes progressively mature into phagolysosomes, which are similar to late endosomes, and then lysosomes. Motor-dependent, bidirectional movement of lysosomes is also shown (Soldati & Schliwa, 2006).

It has been shown that lipid composition and target cell type all influence liposome uptake and trafficking. PERLs are thought to use caveolin- and microtubule-dependent mechanisms to enter the cell as well as the scavenger receptor B1 (SR-B1) and low-density lipoprotein (LDL) receptors (Pollock *et al.*, 2010a). Currently, the only agreed upon statement is the cellular uptake and trafficking mechanism of liposomes is complex and probably multiple mechanisms are at play (Torchilin, 2005). In order to better understand how PERLs enter the cell and traffic to the ER, a systematic approach will be used as described in chapter four. PERLs are made of four phospholipids, PE, PC, PI, and PS; where PE and PC are polyunsaturated. The working hypothesis of this research is that the phospholipid components and the level of unsaturation affect the cellular uptake and mechanisms of endocytosis and the routes and mechanisms of intracellular trafficking.

# Research aims

Although much knowledge has been gained about iminosugars and PERLs, substantial information remains unknown. This research aims to develop crucial quantitative analytical methods for *N*B-DNJ and NAP-DNJ iminosugars in order to compare their encapsulation efficiencies and determine what effect the polarity or hydrophobicity of a chemical compound has, if any, on the encapsulation or incorporation into a liposome as researched in chapter three. This research would also like to decipher the cellular internalisation and intracellular trafficking pathways involved with 'ER-targeting' liposome uptake and movement in vitro, and this is explored extensively in chapter four.

# Chapter two: Methodology

This chapter describes the methods used for the assays described in this research. The HPLC methods are described in chapter 3. The materials information may be found in Appendix B.

## 2.1 Formulation of liposomes using the reverse phase evaporation method

5 mM PERL formulations were made with a ratio of 1.5:1.5:1:1 with the following phospholipids: 22:6 PE, 22:6 PC, 18:1 PI, and 18:1 PS, respectively. 1% Rhodamine lissamine B - PE was included for rhodamine-labeled PERLs. Liposome formulations may be made with other ratios and phospholipids using the same formulation process to achieve the desired formulation. One must consider the phase transition temperature of the target liposome formulation and ensure the appropriate mixing temperature for mixing the lipids is used. Lipid stock solutions were placed into glass vials with organic resistant septa and caps and the lipid suspension was evaporated under a stream of nitrogen gas whilst constantly rotating the vial. The lipid mixture was re-suspended into the appropriate volume of phosphate buffer saline (PBS), calcein solution, or iminosugar solutions of various concentrations. The suspensions were then vortexed for 1-3 hours. MERL and PERL formulations may be vortexed at room temperature. The resulting multilamellar vesicles (MLVs) were extruded 11 times through a mini-extruder device with a polycarbonate 100 nm pore diameter filter with two micromembrane filter supports. Formulations were stored at 4°C.

## 2.2 Separation of liposomes from free calcein/un-encapsulated drug

Sephadex G-50 (medium) size exclusion resin was swollen in the same buffer as the liposomes were formulated with according to the manufacturer's instructions. Disposable chromatography columns were packed with the Sephadex G-50 (medium) slurry. The columns were centrifuged for three minutes at 2000 x g (rcf) to remove excess buffer from the gel. The size exclusion columns were then transferred to fresh tubes and 100 µl of the liposome preparation was added carefully to the top of the size exclusion column bed one drop at a time. The columns were centrifuged for ten minutes at 50 x g with liquid remaining on the column. An additional three-minute centrifugation step at 2000 x g was performed to expel liposomal material from the column into the tube. The calcein or un-encapsulated drug remained in column. The column was transferred to a fresh falcon tube. In order to recover the non-encapsulated calcein from the column, 1ml of the buffer used to prepare the Sephadex resin was be added to the column followed by 2000 x g centrifugation for three minutes. The non-encapsulated samples may be analyzed by high performance liquid chromatography (HPLC) depending of the mode of detection. The encapsulated samples will need further extraction to remove the encapsulated contents from the liposomes for downstream quantitative analysis.

# 2.3 Compound extraction from liposomes and solid phase extraction to remove lipids from the sample matrix

### 2.3.1 Compound extractions

The compound extraction buffer (1% Triton X-100 or 10, 50, or 100% methanol or ethanol solution) was added to the liposome formulation containing an iminosugar in a 1:1 ratio. The sample was then vortexed and incubated at ambient conditions for 1 hour.

The percent recovery is determined by the following calculation:

$$\mathbf{( C_f / C_i ) \times 100 = Percent\ recovery\ (\%)}$$

Where $C_f$ is the final concentration determined analytically by HPLC compared to an internal standard and $C_i$ is the intial concentration of the drug in the liposome formulation. All dilutions and changes in volume were accounted for throughout the purfication process.

### 2.3.2 Solid phase extraction of lipids from sample matrix

Varian Bond Elut strong cation exchange SCX columns 100 mg, 1ml were used by gravity flow. The columns were preconditioned by adding methanol to the top of the column and allowing elution under gravity. 1M hydrochloric acid was added to the sample to yield a final concentration of 50 mM and then vortexed. The sample was then added drop wise to the column bed. The column was filled to the top with water and allowed to elute under gravity. The eluant was then discarded. The column was

transferred to a new falcon tube and 1 ml 1% ammonia/methanol was added to each column and allowed to elute under gravity. This eluant is kept and dried under nitrogen.

## 2.4 Calcein encapsulation determination

1 to 10 µl of liposomes or free calcein fractions were added to 2 ml 2-[[1,3-dihydroxy-2-(hydroxymethyl)propan-2-yl]amino]ethanesulfonic acid (TES) buffer, pH 7 which had been pre-warmed to 37 ºC. The 3 x 200 µl replicates were placed into a 96-well plate for fluorescence analysis at $\lambda_{ex}$ = 490 nm and $\lambda_{em}$ = 520 nm at 30 minute intervals for up to one hour. 2 µl 10% Triton X-100 was added to each well and incubated for 10 min with stirring. The final fluorescence measurement was taken using $\lambda_{ex}$ = 490 nm and $\lambda_{em}$ = 520 nm. The percent encapsulation efficiency was calculated by comparing free calcein to entrapped liposomes. The following equation was used to determine the encapsulation efficiency in liposomes:

$$R_r = 100 \times ((I_t - I_0) / (I_\infty - I_0))$$

$R_t$ = extent of release

$I_t$ = Intensity at time t, (ex: 30, 60, 90, 120, 150, 180, etc minutes)

$I_0$ = Initial fluorescence at initial time point

$I_\infty$ = final fluorescence achieved by lysing liposomes

## 2.5 Cell culture

Adherent Huh7.5 cells (a gift from C. Rice, Rockefeller University) were grown in complete Dulbecco's modified essential media (DMEM) (100 U/ml penicillin, 100 µg/ml

streptomycin, 2 mM L-glutamine, 1x modified essential media, MEM) with 10% FBS prior to experiments. Imaging experiments used phenol-red free DMEM. All incubations were at 37°C / 5% $CO_2$ unless otherwise stated. Cells were passaged 1:5 dilution, three times per week.

## 2.6 MTS cell toxicity assay

Performed as per manufacturer's protocol, using a Promega CellTiter 96 $AQ_{ueous}$ One Solution Reagent kit. 10,000 cells/ml were seeded and the MTS reagent is incubated with the cells for two hours. Ultraviolet (UV) absorbance readings were then measured at 490 nm. The background UV absorbance (660 nm) was determined and subtracted.

## 2.7 Liposome uptake assays

Rh-PE-labeled liposomes (1% mol) were added to Huh7.5 cells at a final phospholipid concentration of 50 μM in serum-free complete DMEM without phenol red, and left to incubate for 1 hour. For assays in the presence of endocytosis and trafficking inhibitors, each inhibitor was incubated with Huh7.5 cells to determine the concentration leading to 5% cell toxicity by an MTS assay. This inhibitor concentration was then incubated with Huh7.5 cells for 1 hour prior to the addition of Rh-PE-labeled liposomes. Following incubation with liposomes for 1 hour, cells were washed, counted using trypan blue staining, and read in a spectrofluorometer at $\lambda_{ex}$=550 nm, $\lambda_{em}$ =590 nm.

## 2.8 Dynamic light scattering (DLS) analysis of liposomes

A 1:50 liposome formulation in PBS dilution media was made. 50 µL was added to a cuvette specially designed for DLS analysis. The cuvette was then placed in the DLS instrument. The DLS data is acquired with the correct data filter setting selected and the laser properly attenuated within range of the sample. If intensity was too high, the sample was diluted 1:100 with PBS.

# Chapter three: Determination of encapsulation efficiency of iminosugars in endoplasmic reticulum (ER) targeting liposomes

## 3.1 Introduction

In order to dissect the effects of hydrophobicity and polarity on the encapsulation of iminosugars into liposomes, it is crucial that quantitative analytical methods be developed for the iminosugars of interest. Previously, the self-quenching fluorophore calcein was used to determine the encapsulation efficiency of liposomes by lysing the liposomes with Triton X-100 and monitoring the fluorescence before and after lysis (Pollock *et al*., 2010a). This method was used since no quantitative methods for analyzing iminosugars in liposomes had been developed at that point. Since the chemical structure of calcein is quite different to that of any of the iminosugars - as shown in Appendices A1 and A2 - the actual encapsulation efficiencies of iminosugars may not be representative of previously reported encapsulation efficiencies determined by calcein fluorescence assays. The encapsulation efficiencies of the actual iminosugars are required to determine the correct dose ranges for clinical studies.

High performance liquid chromatography (HPLC) with various detection modes were used to develop robust, quantitative analytical detection for the iminosugars, *N*-Butyl-deoxynojirimycin (*N*B-DNJ) and *N*-6-(*N*'-(4'-azido-2'-nitrophenyl)amino)hexyl deoxynojirimycin (NAP-DNJ). Once analytical detection methods are developed for these molecules, the methods will be used to quantify the encapsulation efficiency of each type of iminosugar in liposomal formulations.

The two iminosugars, *N*B-DNJ and NAP-DNJ, were selected to serve as models to elucidate the different mechanisms and chemical properties involved in small molecules becoming encapsulated into 'ER-targeting' liposomes. The chemical substitution of the endocyclic nitrogen atom varies substantially between the iminosugars, since *N*B-DNJ has a substituted four-carbon alkyl chain and NAP-DNJ has a longer, more elaborate chain. The hexylbenzyl substitution of the NAP-DNJ structure makes the molecule more hydrophobic than the smaller alkyl chain of *N*B-DNJ. This research aims to use these iminosugar molecules to gain a better understanding of the influence hydrophobicity and polarity have on the incorporation/ encapsulation into liposomes.

*N*B-DNJ does not have a chromophore and therefore cannot be analytically detected using ultraviolet (UV) detection. Since *N*B-DNJ was previously detected (Mellor *et al.*, 2000) with HPLC coupled with pulsed amperometric detection (PAD) this was the first analytical detection method used to determine the encapsulation efficiency of *N*B-DNJ in 'ER-targeting' liposomes.

*Pulsed Amperometric Detection*

The presence of hydroxyl groups in the iminosugar ring should allow carboxyanion formation at high pH and detection using PAD. Cation-exchange chromatography was used to separate the iminosugars from each other and any other components of the sample matrix. Because PAD requires the eluant to be basic, the acidic eluant that exits the cation exchange column is exchanged using a micromembrane suppressor using water as the regenerant.

Carbohydrates are detected by measuring the electrical current generated by their oxidation at the surface of a gold electrode. The products of this oxidation reaction also poison the surface of the electrode, which means that it has to be cleaned between measurements. This is accomplished by first raising the potential to a level sufficient to oxidize the gold surface. This oxidation causes desorption of the carbohydrate oxidation products. The electrode potential is then lowered to reduce the electrode surface back to gold. The sequence of potentials is illustrated in Figure 4. PAD employs a repeating sequence of three potentials. Current integrated over time is charge, so the detector response is measured in coulombs and the average current during the integration period can be reported in amperes.

**Figure 4: Diagram of the pulse sequence to detect carbohydrates using PAD (Dionex Corporation, 2000).**

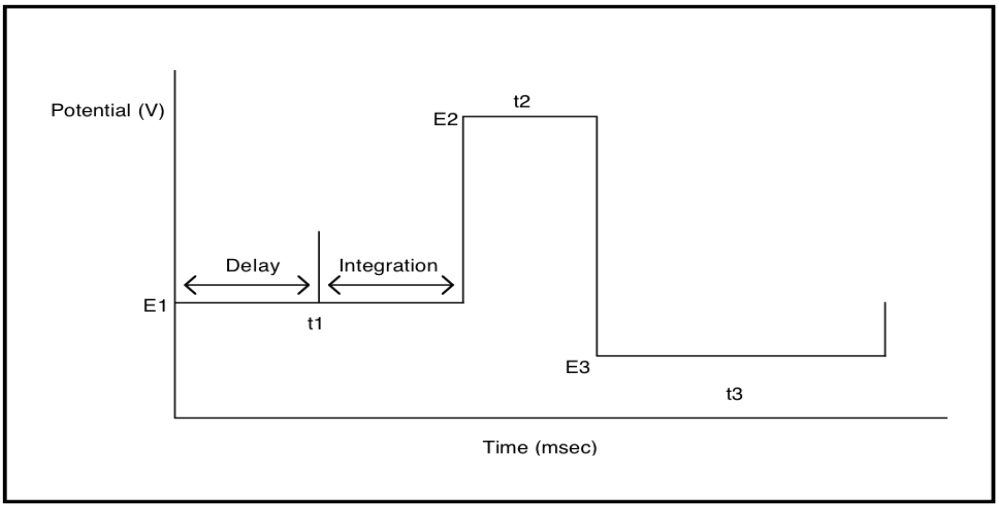


PAD uses a repeating sequence of three potentials. Current from carbohydrate oxidation is measured at the first potential, $E_1$. The second, $E_2$, is a more positive potential that oxidizes the gold electrode and cleans it of products from the carbohydrate oxidation. The third potential, $E_3$, reduces the gold oxide on the electrode surface back to gold, thus permitting detection during the next cycle at $E_1$.The three potentials are applied for fixed durations referred to as $t_1$, $t_2$, and $t_3$ (Dionex Corporation, 2000).

If the pulsed amperometric detection is not capable of quantitative analysis of *N*B-DNJ in 'ER-targeting' liposomes, refractive index detection is another detection method that may be employed for this purpose.

*Refractive Index Detection (RID)*

The theory behind refractive index detection is well understood. When a beam of light passes from one medium into another, the wave velocity and direction changes. The change in direction is called refraction. The relationship between the angle of incidence and the angle of refraction is expressed in Snell's Law of refraction as shown in Equation 1.

**Equation 1: Snells's Law**

$$n = \frac{n_2}{n_1} = \frac{\sin\alpha_1}{\sin\alpha_2}$$

Where:

n = Refractive index of medium 1 relative to medium 2

$n_2$ = Refractive index of medium 2

$n_1$ = Refractive index of medium 1

$\alpha_1$ = angle of incident light in medium 1

$\alpha_2$ =angle of refraction in medium 2

By comparing the angle of diffraction of a solution containing an analyte of interest with the angle of diffraction of the solvent alone, a concentration-dependent response can be plotted from the difference in angles of refraction of the two solutions.

HPLC with ultraviolet detection (HPLC-UV) will be employed to detect NAP-DNJ using reverse-phase (RP) chromatography. The nitrophenyl conjugated pi system of NAP-DNJ causes an electric excitation transition when hit by UV light allowing for UV detection. The nitrophenyl group also creates a dipole moment allowing this property to be exploited by reverse-phase chromatography. A combination of HPLC-UV, PAD, and RID will hopefully yield robust, quantitative detection for each iminosugar in liposome formulations.

## 3.2 Experimental design

The overview of the experimental design for this study is described in Table 5. The main objectives were to repeat a previous study that determined the encapsulation efficiency of calcein in 'ER-targeting' liposomes using fluorescence, to develop quantitative analytical methods for the iminosugars in liposomes, *in situ*, and to optimize the sample preparation and extraction conditions required for simultaneous analysis of iminosugars and liposomes in order to determine the encapsulation efficiencies quantitatively.

**Figure 5: Experimental overview for determining the encapsulation efficiency of iminosugars in ER-targeting liposomes.**

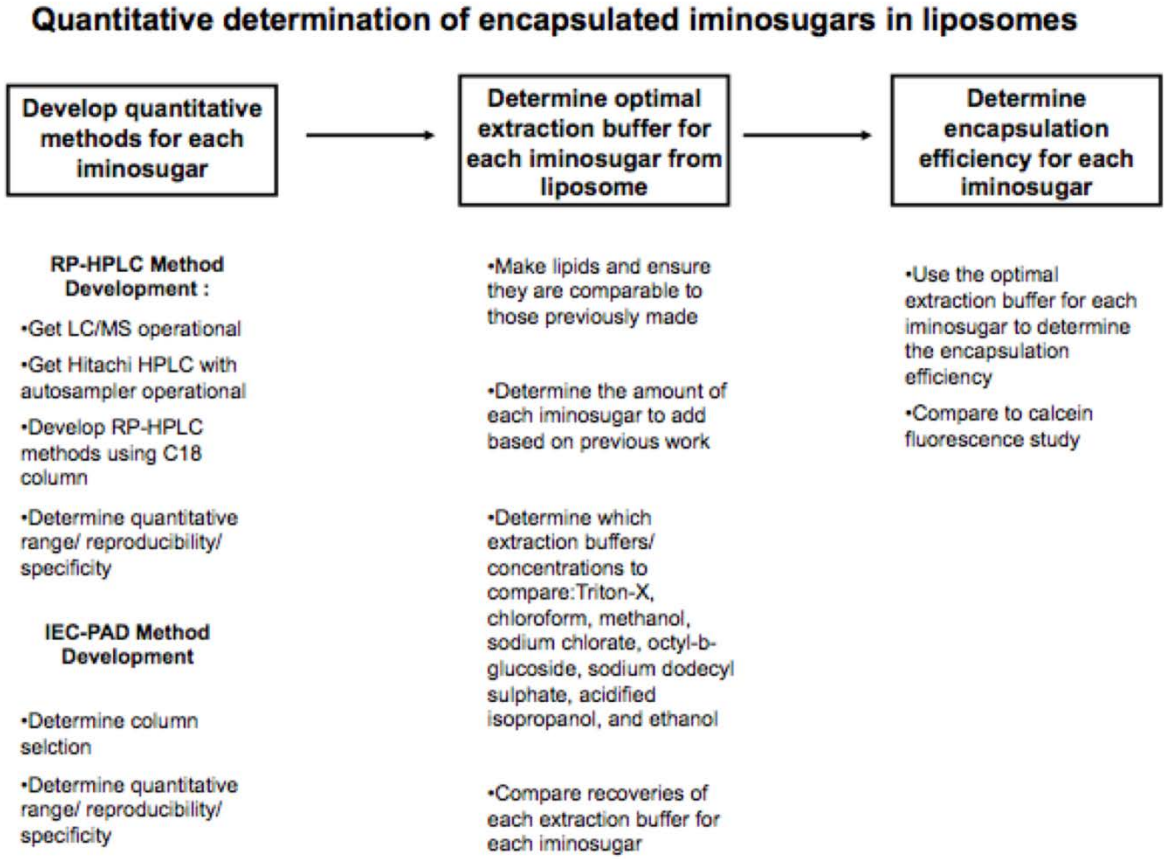


Figure 5: Process for evaluation the encapsulation efficiency of iminosugars in 'ER-targeting' liposomes. Abbreviations: LC/MS liquid chromatography/mass spectrometer, C18 reverse phase chromatography column, IEC-PAD ion exchange chromatography pulsed amperometric detection

## 3.3 Methodology optimized for the determination of the encapsulation efficiencies of iminosugars in liposomes

**Method 1: HPLC-PAD, isocratic; Detection of *N*B-DNJ**

Instrument: Dionex BioLC with an autosampler, quaternary pump, micromembrane suppressor, water regenaration tank, and ED40 pulsed amperometric electrochemical detector (PAD)

Flow rate: 1.0 ml/min

Mobile phase: 2.5 mM sulfuric acid, 50 mM sodium sulfate in 10% acetonitrile

Diluent: deionised $H_2O$

Injection volume: 25 µL

Column: Dionex cation exchange CS-10, 4 x 250 mm

Run time: 15 minutes

**Method 2: HPLC-PAD, gradient; Detection of *N*B-DNJ**

Note: This gradient method was developed to analyze *N*B-DNJ, *N*N-DNJ, *N*B-DGJ, N7-oxadecyl-DNJ, and N9-methoxynonyl-DNJ on the same analytical assay.

Instrument: Dionex BioLC with an autosampler, quaternary pump, micromembrane suppressor, water regenaration tank, and ED40 PAD

Flow rate: 1.0 ml/min

Mobile phase A (MPA): 2.5 mM sulfuric acid, 50 mM sodium sulfate in deionised $H_2O$

Mobile phase B (MPB): 2.5 mM sulfuric acid, 50 mM sodium sulfate in 40% acetonitrile

Diluent: deionised $H_2O$

Injection volume: 25 µL

Column: Dionex cation exchange CS-10, 4 x 250 mm

Gradient:

| Time (min) | %MPB |
|---|---|
| 0 | 2.5 |
| 5 | 2.5 |
| 30 | 100 |
| 35 | 100 |
| 35.1 | 2.5 |
| 50 | 2.5 |

**Method 3: HPLC-RID, isocratic; Detection of *N*B-DNJ**

Instrument: Agilent 1100 with an autosampler, quantenary pump, column oven, refractive index detector (RID)

Flow rate: 1.0 ml/min

Mobile phase: 0.05% triethylamine (TEA), 0.1% trifluoroacetic acid (TFA) in deionised $H_2O$

Diluent: deionised $H_2O$

Injection volume: 50 µL

Column: Zorbax C18, 5 µm, 4.6 x 150 mm

Run time: 5 minutes

**Method 4: HPLC-UV, gradient; Detection of NAP-DNJ**

Instrument: Hitachi LaChrom HPLC with an autosampler, quaternary pump, and diode array detector

Flow rate: 1.5 ml/min

Mobile phase A (MPA): 0.1% formic acid in deionised $H_2O$

Mobile phase B (MPB): 0.1% formic acid in acetonitrile

Diluent: 50/50 acetonitrile/ deionised $H_2O$

Injection volume: 10 µL

Column: Waters Spherisorb 3 µm C18 ODS2 90 Å 50 x 4.6 mm

Detection: 254 nm

Gradient:

| Time (min) | %MPB |
|---|---|
| 0 | 30 |
| 30 | 80 |
| 30.1 | 30 |
| 40 | 30 |

**Method 5: HPLC-UV, gradient; Detection of NAP-DNJ**

Instrument: Agilent HPLC with an autosampler, quaternary pump, and UV detector

Flow rate: 1.5 ml/min

Mobile phase A (MPA): 0.1% formic acid in deonised $H_2O$

Mobile phase B (MPB): 0.1% formic acid in acetonitrile

Diluent: 50/50 acetonitrile/d$H_2O$

Injection volume: 50 µL

Column: Waters Spherisorb 3 µm C18 ODS2 90 Å 50 x 4.6 mm

Detection: 254 nm

Gradient:

| Time (min) | %MPB |
|---|---|
| 0 | 30 |
| 7 | 80 |
| 7.1 | 30 |
| 10 | 30 |

**Calculations for determining the encapsulation efficiency (EE %) and unencapsulation efficiency (UE %)**

Actual mass of the drug/compound is recorded and appropriate volume of diluent is added to achieve the initial target concentration, $C_i$. Example: $M_w$ of *N*B-DNJ is 219.28 g/mol, if 2.21 mg was actually weighed out, 442 µL should be added to produce a $C_i$ of 5 mM. Dilution factors should be recorded and factored in for every process step.

A standard curve made up of standards of the drug of interest at known concentrations would be analyzed on an analytical HPLC to determine the linear equation. The linear equation is calculated by using the chromatographic peak areas determined by integration of the standard chromatographic peaks. This linear equation would used to determine the amount of drug in the samples with unknown amounts of drug such as liposomes samples formulated with the drug of interest. Example: If the standard curve linear equation for *N*B-DNJ is y=438199x+23701 for a standard curve of known *N*B-DNJ concentrations of 50 µM to 50 mM and the integrated *N*B-DNJ peak area of the unknown sample is 147215 AU (absorbance units), the calculated amount would be 16 mM. Finally the total dilution factor should be multiplied by the calculated amount in order to yield the final concentration ($C_f$).

**$(C_f/C_i) * 100$ = Unencapsulation efficiency (UE%)**

**100% - UE% = Encapsulation efficiency (EE%)**

# 3.4 Results

### 3.4.1 Calcein encapsulation efficiency

Thirty-six formulations of 80 mM calcein in 5 mM PERLs were analyzed by the fluorescence detection method described in 2.4 resulting in a mean encapsulation efficiency of 4.26% with a relative standard deviation of 0.17% (data not shown).

### 3.4.2 *N*B-DNJ extraction from liposome sample matrix

80 mM *N*B-DNJ in 5 mM PERLs were formulated in triplicate and incubated with 100 µL of the appropriate extraction buffer at 51°C for 1 hour. The results are shown in Table 1.

**Table 1: Results of study to determine the optimal extraction buffer to be used to extract *N*B-DNJ from PERLs, N = 3.**

| Extraction buffer | Percent recovery (%) |
|---|---|
| 1% Triton X-100 | 70 ± 2.7 |
| 100% water | 49 ± 2.1 |
| 10% methanol | 61 ± 2.8 |
| 50% methanol | 60 ± 2.4 |
| 100% methanol | 53 ± 1.9 |
| 10% ethanol | 48 ± 2.0 |
| 50% ethanol | 46 ± 1.7 |
| 100% ethanol | 34 ± 3.1 |

### 3.4.3 *N*B-DNJ quantitative analysis

Although the linear response of the *N*B-DNJ standard curves when analyzed by the cation exchange chromatography - pulsed amperometric detection system had an acceptable $R^2$ value of 0.999, the system suitability of the sample sets analyzing *N*B-DNJ encapsulated in liposomes was irreproducible. The internal assay standard (1 mM *N*B-DNJ) analyzed before the sample-containing liposomes were injected or analyzed on the cation exchange chromatography - pulsed amperometric system, produced a relative standard deviation of 1.6% for six replicates which is well within the typical acceptable range of <2%. However, the area response of internal standards analyzed throughout the analytical sample set of liposome/ *N*B-DNJ formulations progressively decreased throughout the assay. This rendered the assay results irreproducible and unreliable. The liposomes fouled the gold electrochemical electrode used for PAD analysis, creating a decreased detector response throughout the sample sets. Several cyclic voltammetry pulse sequences were tried in an effort to 'clean' the gold electrode. Although the gold electrode could be cleaned between sample sets, the problem remained between samples and throughout sample sets. This caused the shift to start developing an analytical method using reverse phase chromatography – refractive index detection (RP-RID) for *N*B-DNJ detection. Figure 6 is a sample chromatogram of a *N*B-DNJ standard analyzed by the RP-RID using method 3.

**Figure 6: HPLC-RID chromatogram of *N*B-DNJ using the RP-RID method 3.**

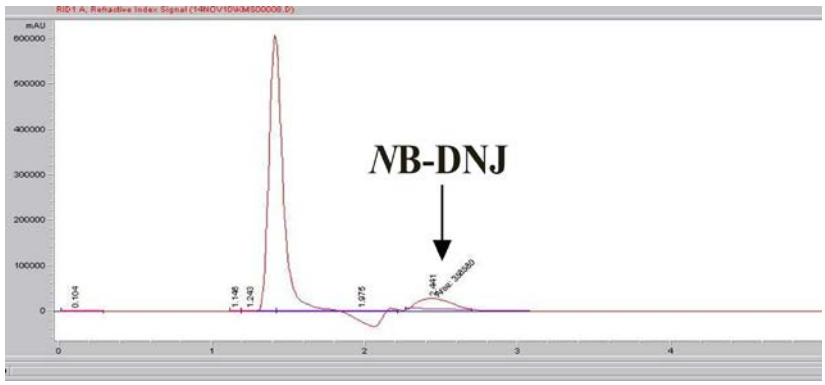


Figure 6 is a HPLC chromatogram of 1 mM *N*B-DNJ analysis with refractive index detection. Initial positive and negative solvent peaks are shown. Y-axis is refractive units (IU) and the x-axis is retention time (minutes). The *N*B-DNJ peak is shown at 2.1 minutes as indicated by the arrow.

The linear range was 500 ng - 2 mg with a linear regression $R^2$ value of 0.998. The limit of detection was 500 ng for *N*B-DNJ using the RP-RID method. However, a new peak coeluted with the *N*B-DNJ peak when *N*B-DNJ in 5 mM PERLs were analyzed as shown in Figure 7.

**Figure 7: HPLC-RID chromatogram showing analysis of 50 mM *N*B-DNJ in 5 mM PERLs using RP-RID method 3.**

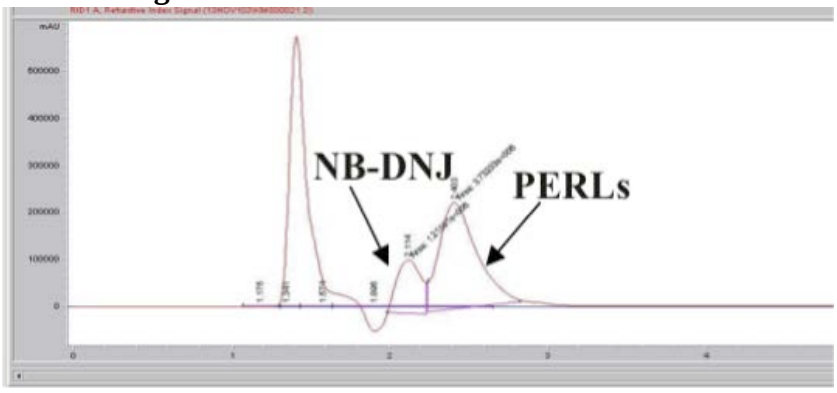


Figure 7 is a HPLC chromatogram of 50 mM *N*B-DNJ in 5 mM PERLs analysis with refractive index detection. Initial positive and negative solvent peaks are shown. Y-axis is refractive units (RU) and the x-axis is retention time (minutes). The *N*B-DNJ peak is shown at 2.1 minutes and the PERLs peak at 2.4 minutes. The integration baseline is shown in purple.

### 3.4.4 Encapsulation of *N*B-DNJ in liposomes

The RP-RID analytical method was used to determine the encapsulation efficiency of *N*B-DNJ in liposomes. The encapsulation efficiency of 1 mM *N*B-DNJ in 5 mM PERLs, n=6, was determined to be 18%, with a standard deviation of 1.5%. The encapsulation efficiency of 1 mM *N*B-DNJ in 10 mM PERLs is 23 ± 2.2%, N=3. A linear range of formulations 100 μM to 100 mM *N*B-DNJ in pH-sensitive liposomes and PERLs were analyzed by the RP-RID analytical method 3 and the encapsulation efficiencies calculated as shown in Table 2. Figure 8 compares the linear regression of the encapsulation efficiency to the concentration of *N*B-DNJ encapsulated in pH-sensitive liposomes and also in PERLs.

**Table 2: Comparing the linearity of the encapsulation efficiency of *N*B-DNJ in 5 mM pH-sensitive liposomes and in 5 mM PERLs determined by the RP-RID method 3. N=6**

| 5 mM liposomes | *N*B-DNJ Encapsulation Efficiency (EE%) | |
|---|---|---|
| | PERLs | pH-sensitive liposomes |
| 100 µM *N*B-DNJ | 22± 2.4% | 26 ± 2.2% |
| 1 mM *N*B-DNJ | 18 ± 1.5% | 18 ± 2.1% |
| 5 mM *N*B-DNJ | 21 ± 2.7% | 23 ± 2.2% |
| 10 mM *N*B-DNJ | 31 ± 3.5% | 41 ± 3.3% |
| 50 mM *N*B-DNJ | 76 ± 5.6% | 71 ± 3.2% |
| 100 mM *N*B-DNJ | 88 ± 6.1% | 74 ± 4.4% |

**Figure 8: Comparing the encapsulation efficiency of *N*B-DNJ in 5 mM pH-sensitive liposomes (blue) and PERLs (green), n=6.**

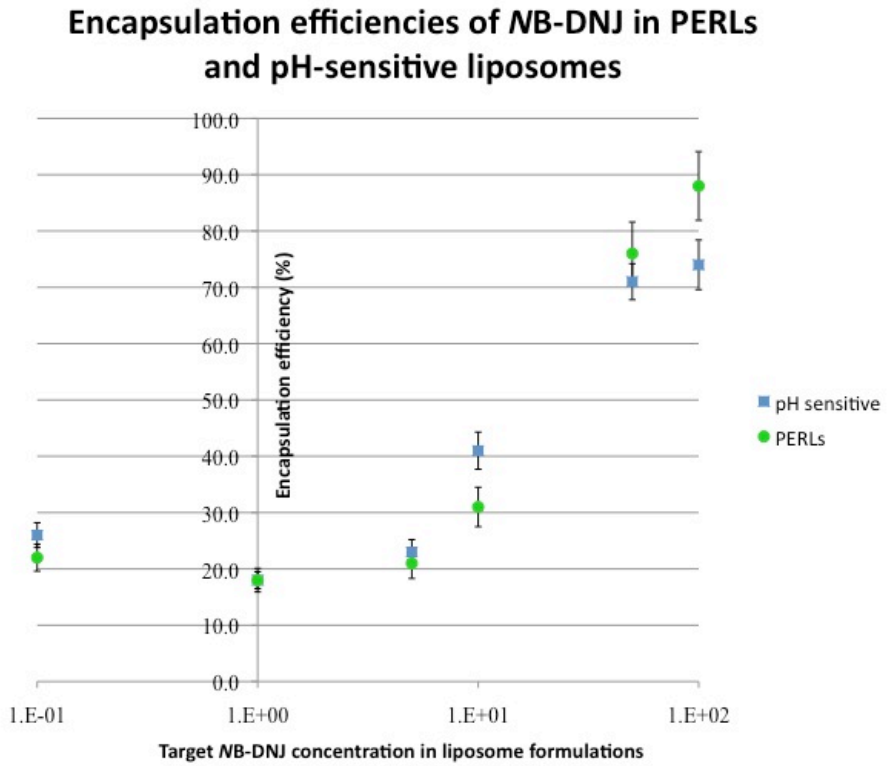


Figure 8 illustrates the encapsulation efficiency of NB-DNJ in pH-sensitive liposomes (pHSLs shown in blue) and polyunsaturated ER-targeting liposomes (PERLs shown in green) for liposome formulations loaded with 0.1 – 100 mM NB-DNJ. The data is presented in logarithmic scale and correlates with the data presented in Table 2. The encapsulation efficiencies were analytically determined by HPLC with refractive index detection with RP-RID method 3. N= 6 for all data points.

### 3.4.5 NAP-DNJ quantitative analysis

Figure 9 is a sample chromatogram of a NAP-DNJ standard analyzed by the reverse phase HPLC ultraviolet detection (RP-UV) method 4.

**Figure 9: HPLC-UV chromatogram of 1 mM NAP-DNJ analyzed by RP-UV method 4.**

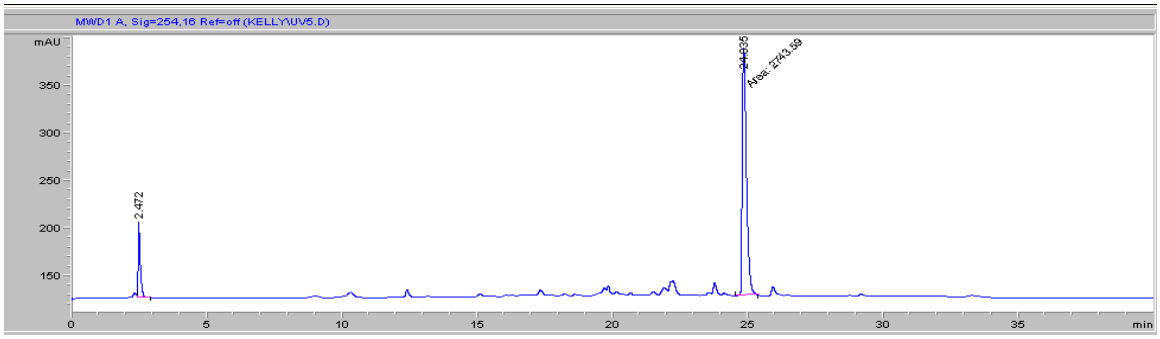


Figure 9 shows the chromatographic trace of 1 mM NAP-DNJ when analyzed by HPLC with UV detection using the long gradient method described in method 4. NAP-DNJ elutes at 25 minutes. The positive solvent front peak is shown. Impurity peaks are observed but are well resolved from the NAP-DNJ peak. Y-axis is absorbance units (AU) and the x-axis is retention time (min). The integration baseline is shown in purple.

The linear range was 100 ng - 4 mg with a linear regression $R^2$ value of 0.999. The limit of detection was 100 ng for NAP-DNJ using the RP-UV detection method. Figure 10 shows a sample chromatogram of NAP-DNJ in 5 mM PERLs when analyzed by the RP-UV detection method 5. Table 3 illustrates the percent recoveries achieved by using various extraction solutions to remove NAP-DNJ from 'ER-targeting' liposomes.

**Table 3: Results of study to determine the optimal extraction buffer to be used to extract NAP-DNJ from PERLs analyzed by RP-UV HPLC method 4, N=3.**

| Extraction buffer | Percent recovery (%) |
|---|---|
| 1% Triton X-100 | 37 ± 3.4 |
| 100% water | 0 ± 0.4 |
| 10% methanol | 12 ± 3.8 |
| 50% methanol | 77 ± 2.2 |
| 100% methanol | 78 ± 2.6 |
| 10% ethanol | 11 ± 2.9 |
| 50% ethanol | 63 ± 3.1 |
| 100% ethanol | 59 ± 2.2 |

**Figure 10: Sample chromatogram of 1 mM NAP-DNJ in 5 mM PERLs formulation analyzed by the gradient RP-UV detection method 5.**

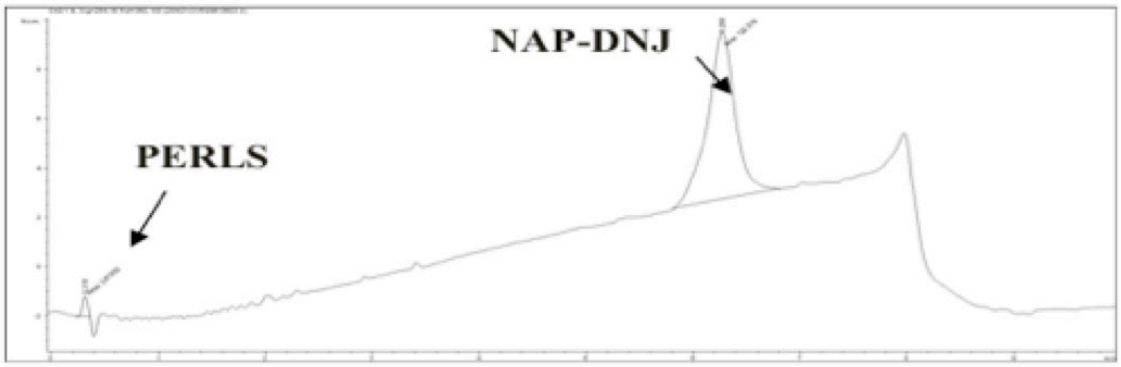


Figure 10 shows the chromatographic trace of 1 mM NAP-DNJ in 5 mM PERLs when analyzed by HPLC with UV detection using a short gradient method described in method 5. The shorter method creates a sharper gradient and peak broadening as can be observed in the chromatogram. NAP-DNJ elutes at 25 minutes while the PERLs elute in the solvent front. The positive solvent front peak is shown. Impurity peaks are observed but are well resolved from the NAP-DNJ peak. Y-axis is absorbance units (AU) and the x-axis is retention time (minutes). The integration baseline is shown in purple.

### 3.4.4 Encapsulation of NAP-DNJ in liposomes

A colleague, Kong Tang, completed an experiment that determined the encapsulation efficiency of 10 µM – 10 mM NAP-DNJ in PERLs. These results are shown in Figure 11.

**Figure 11: The encapsulation efficiencies of NAP-DNJ in PERLs analyzed by the RP-UV method 5, N = 3 (Tang, 2012).**

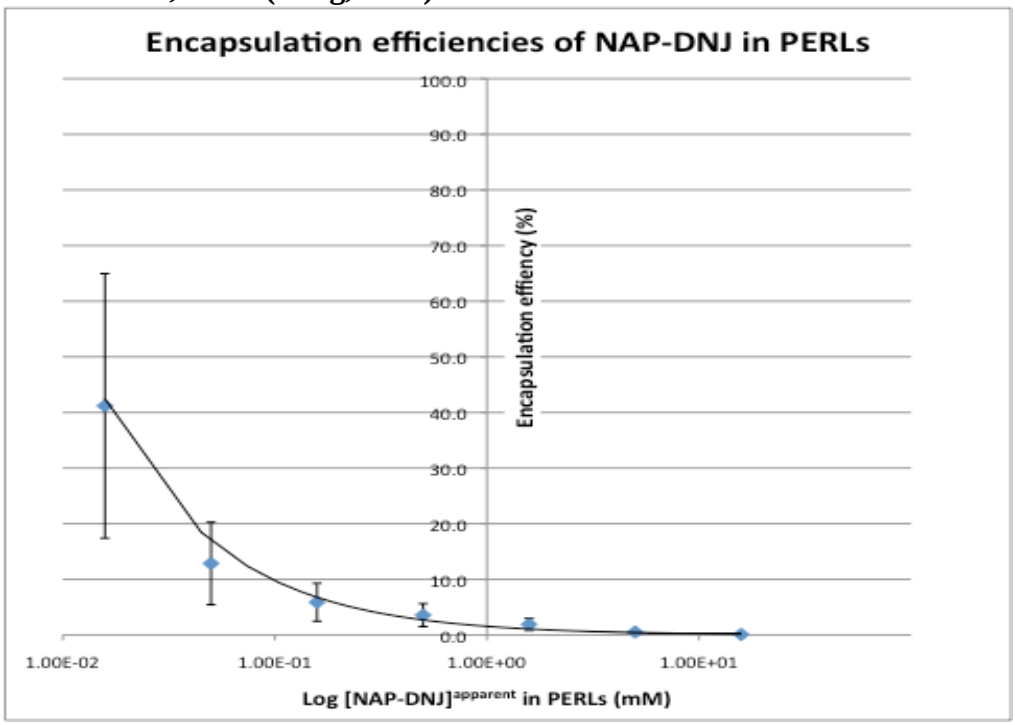


Figure 11 compares the concentration of NAP-DNJ in 5 mM PERL formulations (log mM) to the encapsulation efficiency determined by HPLC analysis using analytical RP-UV method 5, N=3.

## 3.5 Discussion

Analytical methods are required to determine the drug delivery efficiency and versatility of 'ER-targeting' liposomes. Iminosugars that inhibit α-glucosidases show promise as therapeutic agents against a broad range of viruses and diseases (Pollock *et al*., 2010b). Liposomes are used to encapsulate iminosugars allowing them to bypass the plasma membrane more readily, potentially resulting in lower doses required for effective antiviral activity with reduced side effects (Hillaireau & Couvreur, 2009). Initially in this study, the optimal extraction solution for removing the iminosugars from liposomes was found to be a 50% methanol solution resulting in 60% recovery of *N*B-DNJ (Table 1) and 77% recovery of NAP-DNJ (Table 3).

This study analyzed and determined the encapsulation efficiency of thirty-six 80 mM calcein in 5 mM PERL formulations to be 4.26% with a relative standard deviation of 0.17% using HPLC with refractive index detection. These results are in line with previous studies using other detection methods to determine the encapsulation efficiency (Pollock *et al*., 2008a; Costin *et al.*, 2002). Although analytical methods had been developed for iminosugars using HPLC-PAD previously (Mellor *et al.*, 2000) this method of detection was not robust when analyzing samples containing liposomes. Although many sample clean up steps were included in the sample preparation to remove the liposomes and lipid components, such as solid phase extraction and C18 cartridge columns, all of the liposome and lipid components could not be removed from the sample matrices causing the irreproducibility. Due to the lack of reproducibility and robustness of the HPLC-PAD when analyzing samples containing liposomes,

alternative detection methods were employed. Next a refractive index detection method utilizing reverse phase chromatography was developed for quantitative analysis of *N*B-DNJ described as method 3. This method was used to determine the encapsulation efficiency of *N*B-DNJ in liposomes. Interestingly, the encapsulation efficiency seems to have a linear response with concentration. A drawback of the HPLC-RID method is the poor peak resolution between the negative peak with a retention time of 2.1 minutes and the *N*B-DNJ peak at 2.4 minutes that becomes difficult to integrate at higher drug concentrations. The samples containing PERLs generated an additional peak that coelutes with the *N*B-DNJ peak creating difficulties in peak integration as illustrated in Figure 7. The individual phospholipids were analyzed and determined not to contribute to the additional peak in the PERL samples. Several analytical columns, analytical HPLC conditions, and sample preparation steps to remove the lipids/liposomes from the sample matrix were tried to improve the peak separation without success. Column coupling of normal phase, reverse phase, and ion exchange columns was also tried with hopes of improving peak resolution but without success. A mass spectrometer method was developed for *N*B-DNJ to check the chromatographic peak purity during method optimization. It is possible that a size exclusion or gel filtration column may be coupled with a reverse or normal phase column in the future to improve peak resolution.

The encapsulation efficiency of 1 mM *N*B-DNJ in 'ER-targeting' and pH-sensitive liposomes was determined to be 18% using refractive index detection coupled with reverse phase chromatography. The encapsulation efficiency of 1 mM NAP-DNJ in 'ER-targeting' liposomes was determined to be 5% using ultraviolet detection coupled with reverse phase chromatography, the encapsulation efficiency increased to 40%

when lower concentrations, 10 µM, were loaded. *N*B-DNJ appeared to have a loading capacity of 80 µM- 80 mM, where 80 mM was the highest concentration attempted. NAP- DNJ had a loading capacity of 10 µM – 2 mM; NAP-DNJ concentrations above 2 mM appeared to precipitate out of solution. This may be due to the differing solubility of each compound since *N*B-DNJ is highly soluble in aqueous solutions, whereas NAP-DNJ has limited solubility in aqueous solutions but is soluble in organic solvents such as DMSO. This study shows the encapsulation efficiency to be similar for *N*B-DNJ and NAP-DNJ at a 1 mM concentration in 5 mM PERL formulation, but the iminosugars have different behavior at higher concentrations. This suggests that hydrophobicity plays a larger role in the ability of a compound to become incorporated or encapsulated into the lipid bilayer structure of a liposome rather than polarity. This may be due to polar properties of the lipid bilayer of the liposomes allowing the iminosugar compounds to interact readily with the polar phospholipid head groups. *N*B-DNJ appeared to have a wider concentration range at which it could be encapsulated into liposomes than NAP-DNJ. This is likely to be because of the decreased hydrophobic properties of *N*B-DNJ. This information should be considered when developing the formulation processes to encapsulate iminosugars into liposomes.

There are several other N-alkylated DNJ analogues - such as the ones shown in Appendix A1 - that may be encapsulated in liposomes for enhanced drug delivery, and similar methods using reverse phase chromatography combined with refractive index detection may be used to determine their encapsulation efficiencies in the future. pH-sensitive liposomes and PERLs were the only types of liposomal formulations used to encapsulate these iminosugars. It would be interesting to see how the encapsulation

efficiency varies in response to different phospholipid components of other liposome types. There are several methods other than the reverse phase evaporation method used here to formulate liposomes that could change or improve the drug loading encapsulation efficiency and could be looked at to enhance the encapsulation efficiency of iminosugars into liposomes (Riaz, 1996). The knowledge gained about the encapsulation efficiencies of *N*B-DNJ and NAP-DNJ in 'ER-targeting' liposomes will be helpful when designing dosing regimes and determining dosing ranges for future clinical studies.

# Chapter four: Cellular uptake and trafficking of endoplasmic reticulum (ER) targeting liposomes

## 4.1 Introduction

Liposomes are commonly used as drug delivery vesicles to enhance the permeation of drugs through the plasma membrane and sometimes to specific organelles. Dissecting how the phospholipid composition affects the cellular entry and trafficking of liposomes is complex. Vesicles 50-300 nm in diameter, such as liposomes, may use caveolae-mediated endocytosis, clathrin-mediated endocytosis, non-clathrin-non-caveolae-dependent endocytosis, phagocytosis, and/or macropinocytosis as cellular internalisation mechanisms (Zaki & Tirelli, 2010). By developing liposomal formulations that avoid clathrin mediated endocytosis and endosomal acidification, the liposome may remain intact through the endosomal pathway meaning lower concentrations of cargo, or drug, may be used to achieve the same effective dose, potentially limiting toxic effects. Avoiding the endosomal pathway could allow the liposomes to have increased stability within the cell with more efficient - and potentially specific - cargo delivery within the cell (Hayer *et al.,* 2010). It is crucial to understand how the liposomes interact with the cellular uptake and trafficking processes in order to design liposomes for optimal drug delivery.

The size, composition, pH, polarity, isoelectric charge, and stability are the main features of a liposome that affect its mode of cellular internalisation and movement (Torchillin, 2005). The main components of a phospholipid that may affect cellular entry and trafficking are the head group chemistry and the fatty acid saturation and length (see Appendix A3). A recent publication (Pollock *et al.,* 2010a) showed that monounsaturated liposome formulations containing phosphatidylinositol, PI, and phosphatidylserine, PS, increase the colocalization with the ER marker, EDEM, in Huh7.5 cells as shown in Figure 12.

**Figure 12: Colocalization of Rh-PE-labeled liposomes with ER marker, EDEM, in Huh7.5 cells using confocal microscopy (Pollock, 2010a).**

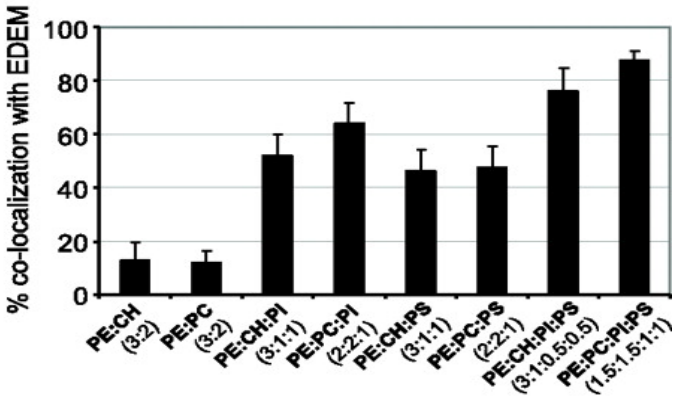


Figure 12: Calculated colocalization of liposome-delivered rh-PE with the EDEM antibody. Results represent mean sd colocalization for 30 cells analysed.

Figure 13 is an illustration of the many cellular endocytosis and trafficking mechanisms and the inhibitors used in this study to alter them.

**Figure 13: Inhibitors of endocytosis and intracellular trafficking mechanisms (adapted from Pollock, 2008).**

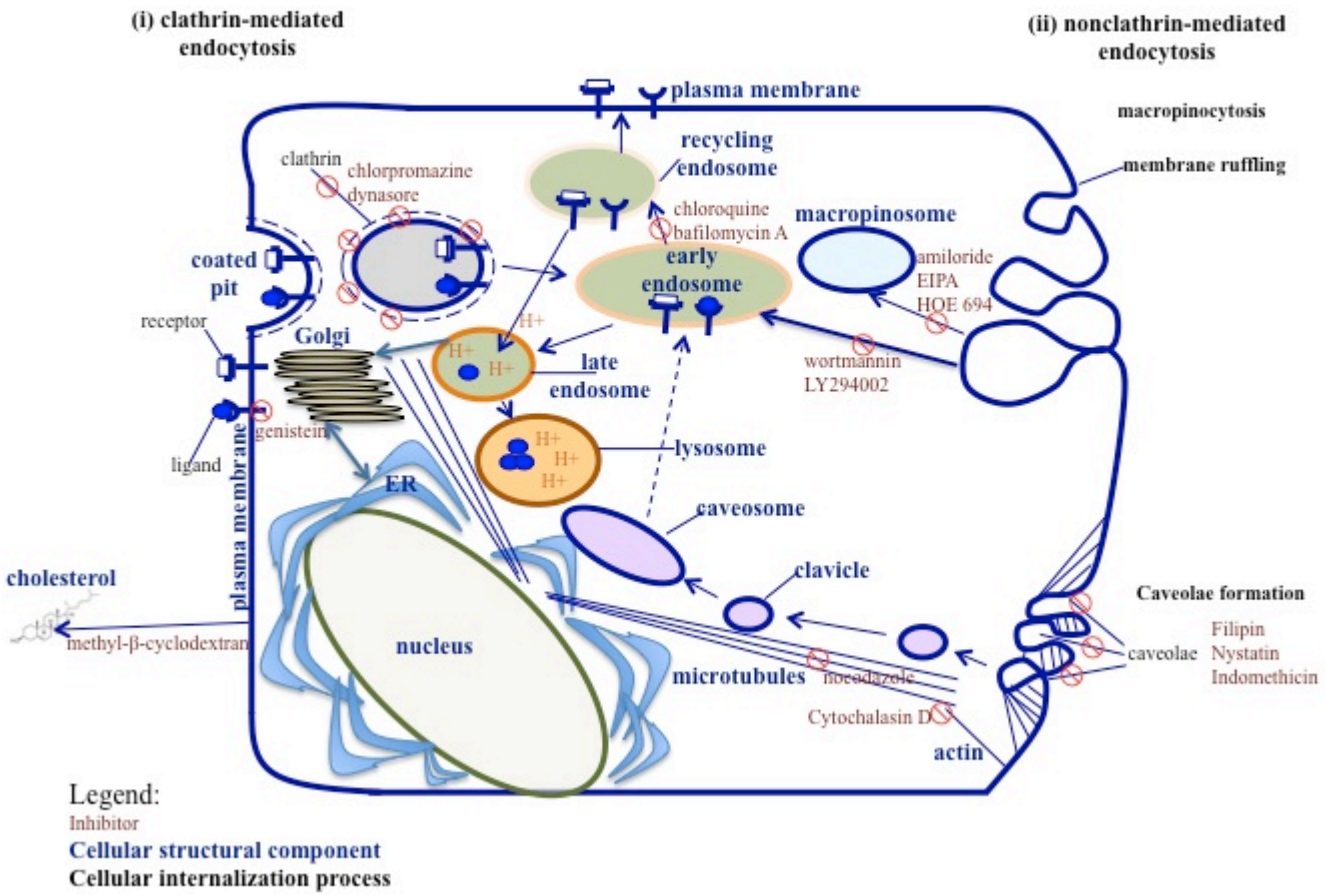

A summary of the literature search for the cellular internalisation and/or cellular trafficking inhibitors is included in Table 4.

**Table 4: 16 inhibitors of endocytosis and intracellular trafficking mechanisms used in this study to identify the cellular endocytosis and trafficking pathways affected by liposomes with various concentrations of phospholipids (2 pages).**

| Cellar process | Inhibitor | Inhibition process | Reference | Literature recommended concentration |
|---|---|---|---|---|
| Caveolae | Filipin | binding to 3b-hydroxysterols | Manunta *et al.*, 2006 | 5 µg/ml |
| | Indomethacin | nonselective inhibitor of cyclooxygenase (COX) 1 and 2, enzymes that participate in prostaglandin synthesis from arachidonic acid | Yumoto *et al.*, 2006 | 75–300 µM |
| | Nystatin | binding to 3b-hydroxysterols | Manunta *et al.*, 2006 | 10 µM |
| Clathrin | Chlorpromazine | inhibitor of clathrin-coated pit formation at the plasma membrane | Götte *et al.*, 2004 | 12 µM |
| | Methyl-β-cyclodextrin (MβCD) | cyclic oligomer of glucopyranoside that inhibits cholesterol-dependent endocytic processes by reversibly extracting the steroid out of the plasma membrane | Thomsen *et al.*, 2002 | 4 mmol/l |
| | Genistein | tyrosine kinase inhibitor shown previously to inhibit clathrin-independent internalisation of a variety of ligands, including CTB | Zaki and Tirelli, 2010 | 400 µmol/l or 40 mM |
| | Dynasore | inhibitor of dynamin I and dynamin II, prevents clathrin coat formation | Macia *et al.*, 2006 | 15, 80 µM |

Table 4 continued: 16 inhibitors of endocytosis and intracellular trafficking mechanisms used in this study to identify the cellular endocytosis and trafficking pathways affected by liposomes with various concentrations of phospholipids.

| **Cellar process** | **Inhibitor** | **Inhibition process** | **Reference** | **Literature recommended concentration** |
|---|---|---|---|---|
| Macropinocytosis | Amiloride | inhibitor of Na+/H+ exchangers, inhibit protein kinase-C | Parton, 2004 | 100 µM |
| | Wortmannin | inhibits PI3K, inhibits the formation of endosomes | Arcaro and Wymann, 1993 | 10 nM |
| | HOE 694 | inhibitor of Na+/H+ exchanger isoform, more selective | Koivusalo *et al.*, 2010 | 10 µM |
| | EIPA | inhibitor of $Na^+/H^+$ exchanger, NHE1 | Koivusalo *et al.*, 2010 | 75 µM |
| | LY 294002 | inhibits PI3K | Corvera and Czech, 1998 | 20, 29 µM |
| Endosomal acidification | Chloroquine | acidification-induced endosomal escape and may inhibit receptor recycling | Dijkstra *et al.*, 1984 | 200 µM |
| | Bafilomycin A | acidification-induced endosomal escape and may inhibit receptor recycling | Issa *et al.*, 2006 | 200 nM |
| Actin | Cytochalasin D | actin filament barbed-end capping | Qaddoumi *et al.*, 2004 | 1 µM |
| Microtubules | Nocodazole | interfering with the polymerization of microtubules | Parton, 2004 | 1.5 µg/ml or 5 nM |

Table 4 oversimplifies the effects of the inhibitors on cellular processes and only describes the main effect. Many of the inhibitors have known multiple effects on cellular endocytosis and/or trafficking processes. Even when only one inhibitor is present, several cellular processes may be affected that are difficult to elucidate when compounded. Many of the mechanisms in which the inhibitors affect the cellular processes are not yet fully understood.

Pollock *et al.* (2010a) used several types of selective inhibitors of cellular uptake/ endocytosis pathways to treat Huh7.5 cells where rhodamine labelled monounsaturated ER-targeting liposomes were added to dissect the pathways involved in the cellular internalisation and trafficking of the monounsaturated liposomes containing PC, PE, PI, and PS in a 1.5:1.5:1:1 ratio as illustrated in Figure 14.

**Figure 14: Uptake of 1% rhodamine PE labeled liposomes in the presence of inhibitors of endocytosis and vesicle trafficking in Huh7.5 cells (Pollock *et al.*, 2010a).**

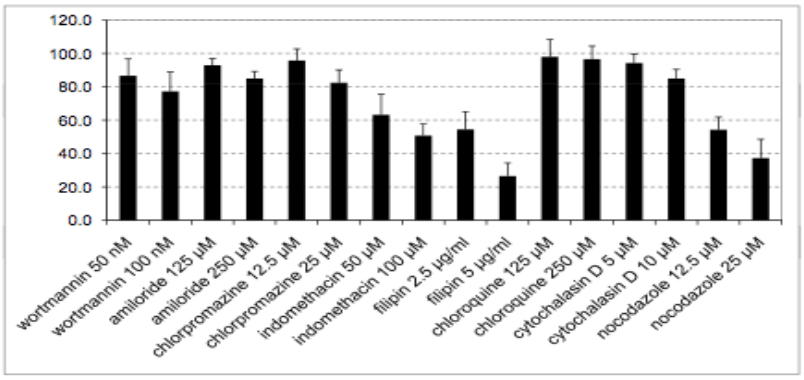


Figure 14: ER liposomes primarily utilize a caveolae-dependent uptake mechanism in combination with scavenger and lipoprotein receptors for entry into target cells. Uptake of 1% rh-PE liposomes in the presence of inhibitors of endocytosis and vesicle trafficking in Huh7.5 cells. Data represent means sd of triplicates from 3 independent experiments. Data are presented in relation to the untreated control (100%) (Pollock *et al.*, 2010a).

This experiment expanded upon this previous research by analyzing the uptake of several rhodamine labelled liposomal formulations in addition to the monounsaturated ER-targeting liposomes, in the presence of the inhibitors used in the recent study (Pollock *et al*., 2010a) and several additional inhibitors in order to identify which phospholipids influence the liposomes' cellular endocytosis and trafficking mechanisms. The methodology used to formulate the liposomes and to determine the amount of uptake of the liposome formulations by fluorescence is described in chapter 2.7.

## 4.2 Experimental design

This study consists of 25 liposome formulations with different phospholipid compositions to identify the influence the phospholipid concentration has on the endocytosis mechanisms involved in the uptake of liposomes into the cell and cellular trafficking. Huh7.5 cells were used since this was the cell line used in a recent study (Pollock *et al.*, 2010) and were readily available and ultimately the only host cells for a robust *in vitro* HCV cell culture system. Considerations for the experimental design of the 25 liposomal formulations with unique attributes:

- Saturated, monounsaturated vs. polyunsaturated phospholipids
- pH-sensitive liposomes (3:2 PE:CHEMS or 3:2 PE:PC) vs. liposomes composed of the 4 phospholipids required for ER colocalization (referred to as 'ER-targeting liposomes') in Huh7.5 cells, PE:PC:PI:PS in varying ratios
- 'ER-targeting liposomes' with higher concentrations of phosphatidylinositol, PI
- 'ER-targeting liposomes' with higher concentrations of phosphatidylserine, PS
- 'ER-targeting liposomes' with equal ratios of PE:PC:PI:PS
- All formulations described in recent publication (Pollock *et al*., 2010a)
- Varying concentrations of tocopherol stabilizer: none, 0.5%, and 1%
- All liposome formulation phospholipids are chemically synthesized
- All liposome formulations will contain 1% Rh-PE to incorporate a fluorescent label
- All liposome formulations will by assayed by dynamic light scattering (DLS) to determine the particle size, homogeneity, and stability of each formulation.

**Table 5: Experimental design for cellular uptake and trafficking of endoplasmic reticulum (ER) targeting liposomes study- 25 formulations with unique phospholipid compositions. The lipids were resuspended in the appropriate diluent volume to yield the final formulation concentration of 5 mM. (See Appendix A1 and 3).**

| Liposome formulations- Endocytosis study – Each formulation contains 1% mmol Rhodamine Lissamine B-PE for fluorescent labelling | | | | | | | | | | | | | | |
|---|---|---|---|---|---|---|---|---|---|---|---|---|---|---|
| **Lipid composition** | **Ratio** | **mmol required per formulation component** | | | | | | | | | | | **Total mmol** | **Strategy** |
| | | **18:1 PE** | **22:6 puPE** | **18:0 dsPC** | **18:1 PC** | **22:6 puPC** | **18:1 PI** | **22:6 puPI** | **18:1 PS** | **22:6 puPS** | **CHEMS** | **Tocopherol** | | |
| PE:PC:PI:PS | 1.5:1.5:1:1 | 1.5 | | | 1.5 | | 1 | | 1 | | | 0.5 | 5.555 | MERLs |
| PE:PC:PI:PS | 1.25:1.25:1.25:1.25 | 1.25 | | | 1.25 | | 1.25 | | 1.25 | | | 0.5 | 5.555 | equal ratios |
| PE:PC:PI:PS | 1:1:2:1 | 1 | | | 1 | | 2 | | 1 | | | 0.5 | 5.555 | 2xPI |
| PE:PC:PI:PS | 1:1:1:2 | 1 | | | 1 | | 1 | | 2 | | | 0.5 | 5.555 | 2xPS |
| PE:PI | 3:2 | 3 | | | | | 2 | | | | | 0.5 | 5.555 | mono PE:PI |
| PE:PS | 3:2 | 3 | | | | | | | 2 | | | 0.5 | 5.555 | mono PE:PS |
| PC:PI:toc | 3:1:1 | | | | 3 | | 1 | | | | | 1 | 5.05 | mono PC:PI |
| PC:PS:toc | 3:1:1 | | | | 3 | | | | 1 | | | 1 | 5.05 | mono PC:PS |
| PC:PI:toc | 3:1:1 | | | 3 | | | 1 | | | | | 1 | 5.05 | sat PC:PI |
| PE:PC:PI:PS | 1.5:1.5:1:1 | | 1.5 | | | 1.5 | | 1 | | 1 | | 0.5 | 5.555 | PERLs |
| PE:PC:PI:PS | 1.25:1.25:1.25:1.25 | | 1.25 | | | 1.25 | | 1.25 | | 1.25 | | 0.5 | 5.555 | equal ratios |
| PE:PC:PI:PS | 1:1:2:1 | | 1 | | | 1 | | 2 | | 1 | | 0.5 | 5.555 | 2xPI |
| PE:PC:PI:PS | 1:1:1:2 | | 1 | | | 1 | | 1 | | 2 | | 0.5 | 5.555 | 2xPS |
| PE:PI | 3:2 | | 3 | | | | 2 | | | | | 0.5 | 5.555 | puPE, PI |
| PE:PS | 3:2 | | 3 | | | | | | 2 | | | 0.5 | 5.555 | puPE, PS |
| PC:PI:toc | 3:1:1 | | | | | 3 | 1 | | | | | 1 | 5.05 | puPC, PI |
| PC:PS:toc | 3:1:1 | | | | | 3 | | | 1 | | | 1 | 5.05 | puPC, PS |
| PC: toc | 4:1 | | | 4 | | | | | | | | 1 | 5.05 | SAI Advantium |
| PE:CHEMS | 3:2 | 3 | | | | | | | | | 2 | | 5.05 | pH sensitive |
| PE:PC | 3:2 | 3 | | | 2 | | | | | | | | 5.05 | *FASEB* rep |
| PE:PI:CHEMS | 3:1:1 | 3 | | | | | 1 | | | | 1 | | 5.05 | *FASEB* rep |
| PE:PC:PI | 3:1:1 | 3 | | | 1 | | 1 | | | | | | 5.05 | *FASEB* rep |
| PE:PS:CHEMS | 3:1:1 | 3 | | | | | | | 1 | | 1 | | 5.05 | *FASEB* rep |
| PE:PC:PS | 3:1:1 | 3 | | | 1 | | | | 1 | | | | 5.05 | *FASEB* rep |
| PE:PI:PS:CHEMS | 1.5:1:1:1.5 | 1.5 | | | | | 1 | | 1 | | 1.5 | | 5.05 | *FASEB* rep |

An MTS or ((3-(4,5-dimethylthiazol-2-yl)-5-(3-carboxymethoxyphenyl)-2-(4-sulfophenyl)-2H-tetrazolium) assay was used to determine the cellular toxicity of the liposomal formulations on Huh7.5 cells following incubation for one hour at the concentrations shown in Table 6. The methodology specifics of the MTS assay are described in Chapter 2.6.

**Table 6: Liposomal formulation concentrations for MTS cellular toxicity assay.**

| 400 µM | 200 µM | 100 µM | 50 µM | 25 µM | 12.5 µM | 6.25 µM |
|---|---|---|---|---|---|---|

The optimal concentration and incubation times of each inhibitor at which the inhibitor is effective at inhibiting its intended cellular pathway or process but is not cytotoxic needs to be determined experimentally. The optimal concentration and incubation time for each of the 16 inhibitors was determined by a literature review as described in Table 4. An MTS assay was used to assess the cell viability of the Huh7.5 cells in the presences of the cellular inhibitors covering a range of inhibitor concentrations and varying incubation times. The optimal inhibitor treatment conditions maintained a cell viability of >95%. The summary of the range of inhibitor concentrations and incubation times to be used for the MTS assay is shown in Table 7. The samples were also visually analyzed on a confocal microscope to observe any major changes to the cellular structure.

**Table 7: The range of optimal cellular endocytosis and trafficking inhibitor concentrations and incubations times to be used for the MTS assay to determine the cellular toxicity in Huh7.5 cells.**

| Inhibitor | Abbreviation | Units | Concentration range | | | | | | | Incubation time |
|---|---|---|---|---|---|---|---|---|---|---|
| Genistein | gen | µmol/l | 8 mM | 800 µM | 80 µM | 8 µM | | | | 120 |
| Wortmannin | wort | nM | 200 | 150 | 100 | 50 | 25 | 20 | 10 | 60 |
| Amiloride | ami | µM | 1000 | 750 | 500 | 250 | 200 | 125 | 100 | 60 |
| Nocodazole | noco | µM | 100 | 50 | 25 | 12.5 | 1000 nM | 100 nM | 10 nM | 60 |
| Chlorpromazine | cz | µM | 100 | 50 | 25 | 12.5 | | | | 60 |
| Chlorpromazine removed | czr | µM | 100 | 50 | 25 | 12.5 | | | | 60 |
| Indomethacin | indo | µM | 400 | 200 | 100 | 50 | | | | 60 |
| Chloroquine | cq | µM | 1000 | 500 | 250 | 125 | | | | 60 |
| Cytochalasin D | cytd | µM | 10 | 5 | 2.5 | 1 | | | | 60 |
| Methyl-β-cyclodextrin (MβCD) | mcd | mM | 20 | 10 | 5 | 1 | | | | 60 |
| Filipin | fil | mg/ml | 20 | 10 | 5 | 2.5 | | | | 60 |
| Bafilomycin A | bafa | nM | 400 | 200 | 100 | 50 | | | | 60 |
| EIPA | eipa | µM | 160 | 80 | 40 | 20 | | | | 60 |
| Genistein | gen | mM/µM | 8 mM | 800 µM | 80 µM | 8 µM | | | | 60 |
| Nystatin | ny | µg/ml | 100 | 50 | 25 | 12.5 | | | | 60 |
| Chlorpromazine | cz | µM | 100 | 50 | 25 | 12.5 | | | | 30 |
| Chlorpromazine removed | czr | µM | 100 | 50 | 25 | 12.5 | | | | 30 |
| Indomethacin | indo | µM | 400 | 200 | 100 | 50 | | | | 30 |
| Chloroquine | cq | µM | 1000 | 500 | 250 | 125 | | | | 30 |
| Cytochalasin D | cytd | µM | 10 | 5 | 2.5 | 1 | | | | 30 |
| Methyl-β-cyclodextrin (MβCD) | mcd | mM | 20 | 10 | 5 | 1 | | | | 30 |
| Filipin | fil | mg/ml | 20 | 10 | 5 | 2.5 | | | | 30 |
| Bafilomycin A | bafa | nM | 400 | 200 | 100 | 50 | | | | 30 |
| HOE 694 | hoe | µM | 80 | 40 | 20 | 10 | | | | 30 |
| LY 294002 | ly | µM | 160 | 80 | 40 | 20 | | | | 30 |
| Nystatin | ny | µg/ml | 100 | 50 | 25 | 12.5 | | | | 30 |
| Nocodazole | noco | µM | 100 | 50 | 25 | 10 | 1000 nM | 100 nM | 10 nM | 30 |
| Dynasore | dyn | µM | 120 | 60 | 30 | 15 | | | | 10 |

Once the optimal concentration/ incubation duration for each inhibitor and the optimal concentration for each liposomal formulation was determined, this information was used to design the experiment to attempt to elucidate the roles the phospholipids have on cellular endocytosis and trafficking. Each of the 16 inhibitors was added with each rh-PE labelled-liposomal formulation (25) on Huh7.5 cells with six technical replicates, three independent experiments for each sample set, and the 96-well plate design accounted for plate bias. Negative controls (for liposome formulations and inhibitors) and blank (media only) were included in each assay. An example of the 96-well plate design is illustrated in Table 8. Two concentrations per inhibitor were used to determine if the inhibitor has a positive or negative effect of liposome uptake. One 96-well plate was required per liposome formulation (25) at one inhibitor concentration, meaning two 96-well plates were required per liposomal formulation. The experimental design includes two 96-well control plates that do not contain any liposome formulations, one plate for each inhibitor concentration (high and low). This experimental design results in fifty-two 96-well plates per independent experiment (3) containing 14,976 samples/controls.

**Table 8: Example of 96-well plate design for rhodamine labeled liposome uptake in Huh7.5 cells in the presence of cellular endocytosis and trafficking inhibitors (one concentration). One 96-well plate per formulation per inhibitor concentration. See Table 7 for abbreviations.**

| | 1 | 2 | 3 | 4 | 5 | 6 | 7 | 8 | 9 | 10 | 11 | 12 |
|---|---|---|---|---|---|---|---|---|---|---|---|---|
| A | cz | cz | cz | cz | cz | cz | indo | indo | indo | indo | indo | indo |
| B | cq | cq | cq | cq | cq | cq | cq | cq | cq | cq | cq | cq |
| C | mcd | mcd | mcd | mcd | mcd | mcd | fil | fil | fil | fil | fil | fil |
| D | bafa | bafa | bafa | bafa | bafa | bafa | hoe | hoe | hoe | hoe | hoe | hoe |
| E | ly | ly | ly | ly | ly | ly | noco | noco | noco | noco | noco | noco |
| F | ny | ny | ny | ny | ny | ny | wort | wort | wort | wort | wort | wort |
| G | ami | ami | ami | ami | ami | ami | eipa | eipa | eipa | eipa | eipa | eipa |
| H | dyn | dyn | dyn | dyn | dyn | dyn | control | control | control | blank | blank | blank |

## 4.3 Results

The assays were completed without any errors, technical or experimental. A typical spectrum from analysis of a liposomal formulation by dynamic light scattering is shown in Figure 15. The cytotoxicity results determined by the MTS assays for the liposome formulations are shown first in Table 9, followed by the cytotoxicity results determined by the MTS assays for the inhibitors in Table 10. The results for the rhodamine labeled liposome uptake assay in Huh7.5 cells in the presence of cellular endocytosis and trafficking inhibitors are shown in Table 11– Table 14. After processing the data and weighing the statistical significance of the results using a 2-tailed Student t test method with a cutoff of $P<0.001$ the results were trended as summarized in Tables Table 11– Table 14 which are split into several tables due to the size of the collated data. The appropriate background fluorescence was subtracted from each sample plate and normalized. The values represent the mean (n=6) percent uptake of liposomes into the Huh7.5 cells. Figure 16 compares uptake of the monounsaturated 'ER-targeting' liposome formulation prepared here with the uptake data presented in a recent study (Pollock *et al.*, 2010a) using the same experimental conditions.

**Figure 15: Analysis of liposomal formulations, 1 and 19, by dynamic light scattering (DLS) analysis.**

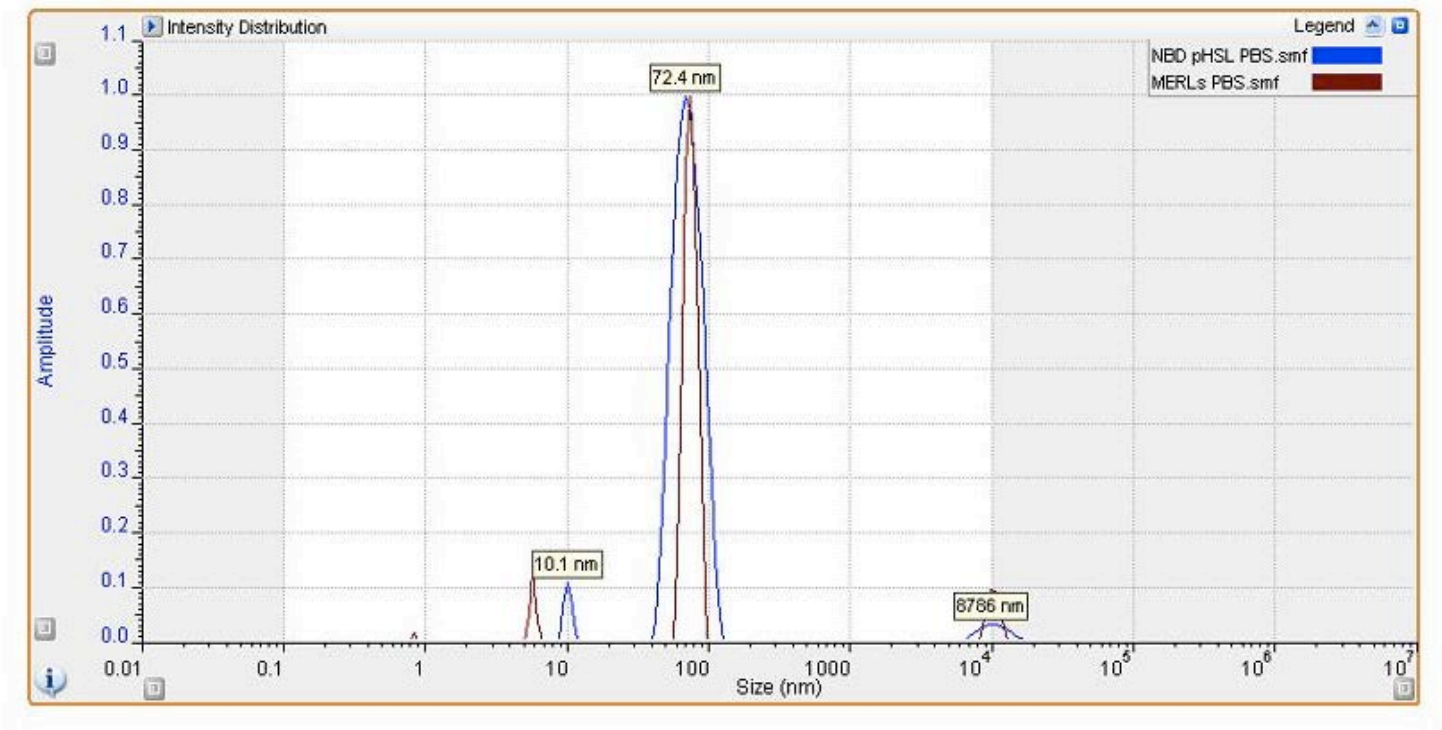


Figure 15: This DLS spectrum is representative of the liposome formulations used in this study. The blue line represents pH-sensitive liposomes, formulation 19, and the red line represents monounsaturated 'ER-targeting' liposomes, formulation 1. The main liposome peak is at 72.4 nm that represents the radii, showing the mean liposome diameter is145 nm in the 100- 200 nm range expected. The peak at the

lower particle size peak at10 nm likely represents impurities and the high particle size peak at 8786 nm is aggregated liposomes observed in the sample matrix.

**Table 9: Highest concentration of each liposome formulation incubated with Huh7.5 cells for 1 hour while maintaining <5% cellular toxicity determined by an MTS assay.**

| Lipid composition | Concentration |
|---|---|
| 18:1 PE:PC:PI:PS | 50 µM |
| 18:1 PE:PC:PI:PS | 50 µM |
| 18:1 PE:PC:PI:PS | 50 µM |
| 18:1 PE:PC:PI:PS | 400 µM |
| 18:1 PE:PI | 100 µM |
| 18:1 PE:PS | 400 µM |
| 18:1 PC:PI:toc | 400 µM |
| 18:1 PC:PS:toc | 400 µM |
| 18:0 PC: 18:1 PI: toc | 50 µM |
| 22:6 PE:PC:PI:PS | 100 µM |
| 22:6 PE:PC:PI:PS | 50 µM |
| 22:6 PE:PC:PI:PS | 400 µM |
| 22:6 PE:PC:PI:PS | 400 µM |
| 22:6 PE: 18:1 PI | 100 µM |
| 22:6 PE: 18:1 PS | 100 µM |
| 22:6 PC: 18:1 PI: toc | 400 µM |
| 22:6 PC: 18:1 PS: toc | 400 µM |
| DSPC: toc | 100 µM |
| 18:1 PE:CHEMS | 100 µM |
| 18:1 PE:PC | 400 µM |
| 18:1 PE:CHEMS:PI | 100 µM |
| 18:1 PE:PC:PI | 100 µM |

**Table 10: Highest concentration of each endocytosis inhibitor incubated for 30 minutes with Huh7.5 cells while maintaining <5% cellular toxicity determined by an MTS assay.**

| Inhibitor | Code | Concentration |
|---|---|---|
| Chlorpromazine | cz | 12.5 µM |
| Indomethacin | indo | 400 µM |
| Chloroquine | cq | 250 µM |
| Cytochalasin D | cytd | 10 µM |
| Methyl-β-cyclodextrin (MβCD) | mcd | 20 mM |
| Filipin | fil | 10 µg/ml |
| Bafilomycin A | bafa | 400 nM |
| HOE 694 | hoe | 40 µM |
| LY 294002 | ly | 80 µM |
| Nocodazole | noco | 25 µM |

| | | |
|---|---|---|
| Nystatin | ny | 50 µg/ml |
| Wortmannin | wort | 200 nM |
| Amiloride | ami | 1 mM |
| EIPA | eipa | 40 µM |
| Dynasore | dyn | 60 µM |

**Table 11: Mean percent uptake of rhodamine labeled liposome formulations in the presence of clathrin and caveolae endocytosis inhibitors. Key Red >110%, 70% < white > 110%, 30% < light green > 70%, dark green < 30% uptake.**

| Mean % uptake of Rh-liposomes in the presence of clathrin or caveolae endocytisis inhibitors (n=6) | | | | | | | | | |
|---|---|---|---|---|---|---|---|---|---|
| **Formulation** | **Internalisation route:** | **Clathrin** | | **Caveolae** | | | | | |
| | **Internalisation inhibitor:** | Chlorpromazine | | Indomethacin | | Filipin | | Nystatin | |
| | **Inhibitor concentration:** | 12.5 µM | 25 µM | 50 µM | 100 µM | 2.5 µg/ml | 5 µg/ml | 12.5 µM | 25 µM |
| **Monounsaturated** | MERLs | 113 | 101 | 88 | 68 | 66 | 34 | 98 | 88 |
| | MERLs equal ratios | 109 | 98 | 86 | 63 | 61 | 32 | 92 | 84 |
| | MERLs 2x PI | 103 | 105 | 68 | 54 | 34 | 22 | 88 | 80 |
| | MERLs 2x PS | 99 | 97 | 96 | 82 | 70 | 48 | 97 | 82 |
| | 18:1 PE:PI | 102 | 103 | 70 | 58 | 45 | 28 | 97 | 92 |
| | 18:1 PE:PS | 96 | 102 | 91 | 84 | 86 | 45 | 86 | 77 |
| | 18:1 PC:PI:toc | 97 | 99 | 71 | 57 | 47 | 22 | 101 | 98 |
| | 18:1 PC:PS:toc | 101 | 94 | 96 | 88 | 68 | 37 | 84 | 71 |
| | 18:0 PC: 18:1 PI: toc | 100 | 99 | 81 | 62 | 51 | 32 | 101 | 99 |
| **Polyunsaturated** | PERLs | 95 | 103 | 92 | 78 | 36 | 16 | 101 | 98 |
| | PERLs equal ratios | 111 | 100 | 88 | 65 | 44 | 21 | 94 | 86 |
| | PERLs 2x PI | 102 | 104 | 67 | 53 | 31 | 18 | 87 | 79 |
| | PERLs 2x PS | 103 | 101 | 100 | 86 | 35 | 20 | 101 | 86 |
| | 22:6 PE: 18:1 PI | 103 | 104 | 71 | 59 | 38 | 20 | 98 | 93 |
| | 22:6 PE: 18:1 PS | 93 | 99 | 88 | 81 | 28 | 14 | 83 | 74 |
| | 22:6 PC: 18:1 PI: toc | 95 | 97 | 69 | 55 | 32 | 19 | 99 | 96 |
| | 22:6 PC: 18:1 PS: toc | 104 | 97 | 99 | 91 | 29 | 17 | 87 | 74 |
| **pH-sensitive** | DSPC: toc | 64 | 31 | 98 | 99 | 49 | 30 | 99 | 97 |
| | 18:1 PE:CHEMS | 62 | 28 | 114 | 108 | 97 | 98 | 107 | 99 |
| | 18:1 PE:PC | 67 | 34 | 106 | 103 | 115 | 101 | 97 | 100 |
| **Pollock et al., 2010a composition** | 18:1 PE:CHEMS:PI | 94 | 96 | 68 | 54 | 44 | 19 | 98 | 95 |
| | 18:1 PE:PC:PI | 101 | 102 | 69 | 57 | 44 | 27 | 96 | 91 |
| | 18:1 PE:CHEMS:PS | 102 | 95 | 97 | 89 | 69 | 38 | 85 | 72 |
| | 18:1 PE:PC:PS | 98 | 104 | 93 | 86 | 88 | 47 | 88 | 79 |
| | 18:1 PE:CHEMS:PI:PS | 110 | 98 | 85 | 65 | 63 | 31 | 95 | 85 |

**Table 12: Mean percent uptake of rhodamine labeled liposome formulations in the presence of cholesterol depletion, dynamin I & II, and actin polymerization inhibitors. Key: Red >110%, 70% < white > 110%, 30% < light green > 70%, dark green < 30% uptake.**

| Mean % uptake of Rh-liposomes in the presence of cholesterol depletion, dynamin I & II, and actin polymerization inhibitors (n=6) | | | | | | | |
|---|---|---|---|---|---|---|---|
| **Formulation** | **Internalisation route:** | **Cholesterol depletion** | | **Dynamin I & II** | | **Actin polymerization** | |
| | **Internalisation inhibitor:** | Methyl-β-cyclodextrin (MβCD) | | Dynasore | | Cytochalasin D | |
| | **Inhibitor concentration:** | 5 mM | 10 mM | 15 µM | 30 µM | 5 µM | 10 µM |
| **Monounsaturated** | MERLs | 80 | 60 | 90 | 95 | 106 | 102 |
| | MERLs equal ratios | 82 | 63 | 91 | 93 | 103 | 99 |
| | MERLs 2x PI | 87 | 71 | 95 | 105 | 102 | 87 |
| | MERLs 2x PS | 82 | 74 | 96 | 92 | 93 | 97 |
| | 18:1 PE:PI | 86 | 70 | 98 | 101 | 105 | 98 |
| | 18:1 PE:PS | 68 | 62 | 88 | 94 | 108 | 102 |
| | 18:1 PC:PI:toc | 78 | 65 | 101 | 100 | 103 | 99 |
| | 18:1 PC:PS:toc | 96 | 82 | 99 | 93 | 99 | 100 |
| | 18:0 PC: 18:1 PI: toc | 95 | 87 | 103 | 99 | 103 | 101 |
| **Polyunsaturated** | PERLs | 23 | 11 | 108 | 103 | 95 | 98 |
| | PERLs equal ratios | 25 | 10 | 93 | 95 | 105 | 101 |
| | PERLs 2x PI | 28 | 12 | 94 | 104 | 101 | 86 |
| | PERLs 2x PS | 29 | 14 | 100 | 96 | 97 | 101 |
| | 22:6 PE: 18:1 PI | 22 | 9 | 99 | 102 | 106 | 99 |
| | 22:6 PE: 18:1 PS | 25 | 16 | 85 | 91 | 105 | 99 |
| | 22:6 PC: 18:1 PI: toc | 29 | 13 | 99 | 98 | 101 | 97 |
| | 22:6 PC: 18:1 PS: toc | 99 | 85 | 102 | 96 | 102 | 103 |
| **pH-sensitive** | DSPC: toc | 93 | 85 | 101 | 97 | 101 | 99 |
| | 18:1 PE:CHEMS | 100 | 99 | 107 | 101 | 102 | 98 |
| | 18:1 PE:PC | 97 | 98 | 102 | 106 | 100 | 98 |
| **Pollock et al., 2010a composition** | 18:1 PE:CHEMS:PI | 75 | 62 | 98 | 97 | 100 | 96 |
| | 18:1 PE:PC:PI | 85 | 69 | 97 | 100 | 104 | 97 |
| | 18:1 PE:CHEMS:PS | 97 | 83 | 100 | 94 | 100 | 101 |
| | 18:1 PE:PC:PS | 70 | 64 | 90 | 96 | 110 | 104 |
| | 18:1 PE:CHEMS:PI:PS | 77 | 57 | 87 | 92 | 103 | 99 |

**Table 13: Mean percent uptake of rhodamine labeled liposome formulations in the presence of endosomal acidification and microtubule inhibitors. Key: Red >110%, 70% < white > 110%, 30% < light green > 70%, dark green < 30% uptake.**

| Mean % uptake of Rh-liposomes in the presence of cholesterol depletion, dynamin I & II, and actin polymerization inhibitors (n=6) | | | | | | | |
|---|---|---|---|---|---|---|---|
| **Formulation** | **Internalisation route:** | **Endosomal acidification** | | | | **Microtubules** | |
| | **Internalisation inhibitor:** | Chloroquine | | Bafilomycin A | | Nocodazole | |
| | **Inhibitor concentration:** | 125 µM | 250 µM | 100 nM | 200 nM | 12.5 µM | 25 µM |
| **Monounsaturated** | MERLs | 105 | 106 | 102 | 103 | 66 | 40 |
| | MERLs equal ratios | 98 | 101 | 97 | 101 | 62 | 38 |
| | MERLs 2x PI | 106 | 102 | 103 | 106 | 40 | 22 |
| | MERLs 2x PS | 104 | 101 | 90 | 94 | 78 | 62 |
| | 18:1 PE:PI | 105 | 101 | 101 | 103 | 45 | 36 |
| | 18:1 PE:PS | 97 | 98 | 91 | 93 | 78 | 60 |
| | 18:1 PC:PI:toc | 99 | 98 | 99 | 101 | 47 | 32 |
| | 18:1 PC:PS:toc | 103 | 101 | 99 | 94 | 61 | 52 |
| | 18:0 PC: 18:1 PI: toc | 102 | 99 | 99 | 101 | 43 | 31 |
| **Polyunsaturated** | PERLs | 101 | 98 | 113 | 105 | 70 | 32 |
| | PERLs equal ratios | 100 | 103 | 99 | 103 | 64 | 40 |
| | PERLs 2x PI | 105 | 101 | 102 | 105 | 39 | 21 |
| | PERLs 2x PS | 108 | 105 | 94 | 98 | 82 | 66 |
| | 22:6 PE: 18:1 PI | 106 | 102 | 102 | 104 | 46 | 37 |
| | 22:6 PE: 18:1 PS | 94 | 95 | 88 | 90 | 75 | 57 |
| | 22:6 PC: 18:1 PI: toc | 97 | 96 | 97 | 99 | 45 | 30 |
| | 22:6 PC: 18:1 PS: toc | 106 | 104 | 102 | 97 | 64 | 55 |
| **pH-sensitive** | DSPC: toc | 100 | 97 | 97 | 99 | 41 | 29 |
| | 18:1 PE:CHEMS | 119 | 106 | 106 | 104 | 110 | 97 |
| | 18:1 PE:PC | 97 | 101 | 88 | 99 | 128 | 102 |
| **Pollock et al., 2010a composition** | 18:1 PE:CHEMS:PI | 96 | 95 | 96 | 98 | 44 | 29 |
| | 18:1 PE:PC:PI | 104 | 100 | 100 | 102 | 44 | 35 |
| | 18:1 PE:CHEMS:PS | 104 | 102 | 100 | 95 | 62 | 53 |
| | 18:1 PE:PC:PS | 99 | 100 | 93 | 95 | 70 | 62 |
| | 18:1 PE:CHEMS:PI:PS | 102 | 103 | 99 | 100 | 63 | 37 |

**Table 14: Mean percent uptake of rhodamine labeled liposome formulations in the presence of micropinocytosis inhibitors. Key: Red >110%, 70% < white > 110%, 30% < light green > 70%, dark green < 30% uptake.**

| Mean % uptake of Rh-liposomes in the presence of micropinocytosis inhibitors (n=6) | | | | | | | | | | | |
|---|---|---|---|---|---|---|---|---|---|---|---|
| **Formulation** | **Internalisation route:** | **Macropinocytosis** | | | | | | | | | |
| | **Internalisation inhibitor:** | HOE 694 | | LY 294002 | | Wortmannin | | Amiloride | | EIPA | |
| | **Inhibitor concentration:** | 10 µM | 40 µM | 20 µM | 40 µM | 50 nM | 100 nM | 125 µM | 250 µM | 10 µM | 20 µM |
| **Monounsaturated** | MERLs | 87 | 73 | 78 | 62 | 101 | 86 | 107 | 100 | 91 | 72 |
| | MERLs equal ratios | 82 | 65 | 75 | 58 | 98 | 82 | 99 | 102 | 86 | 68 |
| | MERLs 2x PI | 78 | 69 | 51 | 28 | 94 | 92 | 100 | 91 | 72 | 66 |
| | MERLs 2x PS | 74 | 45 | 84 | 78 | 95 | 97 | 89 | 78 | 61 | 35 |
| | 18:1 PE:PI | 98 | 101 | 48 | 31 | 97 | 98 | 101 | 98 | 97 | 101 |
| | 18:1 PE:PS | 68 | 38 | 104 | 98 | 90 | 99 | 73 | 62 | 40 | 18 |
| | 18:1 PC:PI:toc | 99 | 103 | 44 | 29 | 98 | 94 | 99 | 102 | 101 | 99 |
| | 18:1 PC:PS:toc | 60 | 28 | 83 | 82 | 104 | 97 | 81 | 71 | 43 | 38 |
| | 18:0 PC: 18:1 PI: toc | 97 | 102 | 41 | 27 | 103 | 101 | 98 | 98 | 95 | 102 |
| **Polyunsaturated** | PERLs | 98 | 92 | 82 | 72 | 112 | 98 | 105 | 101 | 100 | 98 |
| | PERLs equal ratios | 84 | 67 | 77 | 60 | 100 | 84 | 101 | 104 | 88 | 70 |
| | PERLs 2x PI | 77 | 68 | 50 | 27 | 93 | 91 | 99 | 90 | 71 | 65 |
| | PERLs 2x PS | 78 | 49 | 88 | 82 | 99 | 101 | 93 | 82 | 65 | 39 |
| | 22:6 PE: 18:1 PI | 99 | 102 | 49 | 32 | 98 | 99 | 102 | 99 | 98 | 102 |
| | 22:6 PE: 18:1 PS | 65 | 35 | 101 | 95 | 87 | 96 | 70 | 59 | 37 | 15 |
| | 22:6 PC: 18:1 PI: toc | 97 | 101 | 42 | 27 | 96 | 92 | 97 | 100 | 99 | 97 |
| | 22:6 PC: 18:1 PS: toc | 63 | 31 | 86 | 85 | 107 | 100 | 84 | 74 | 46 | 41 |
| **pH-sensitive** | DSPC: toc | 95 | 100 | 39 | 25 | 101 | 99 | 96 | 96 | 93 | 100 |
| | 18:1 PE:CHEMS | 103 | 102 | 104 | 101 | 106 | 104 | 97 | 103 | 112 | 103 |
| | 18:1 PE:PC | 97 | 103 | 97 | 98 | 77 | 75 | 106 | 102 | 116 | 99 |
| **Pollock et al., 2010a composition** | 18:1 PE:CHEMS:PI | 96 | 100 | 41 | 26 | 95 | 91 | 96 | 99 | 98 | 96 |
| | 18:1 PE:PC:PI | 97 | 100 | 47 | 30 | 96 | 97 | 100 | 97 | 96 | 100 |
| | 18:1 PE:CHEMS:PS | 61 | 29 | 84 | 83 | 105 | 98 | 82 | 72 | 44 | 39 |
| | 18:1 PE:PC:PS | 70 | 40 | 106 | 100 | 92 | 101 | 75 | 64 | 42 | 20 |
| | 18:1 PE:CHEMS:PI:PS | 84 | 70 | 75 | 59 | 98 | 83 | 104 | 97 | 88 | 69 |

**Figure 16: Comparison of uptake of rhodamine labeled monounsaturated 'ER-targeting' liposome data from this experiment to the data observed for the previously published data (Pollock *et al*., 2010a).**

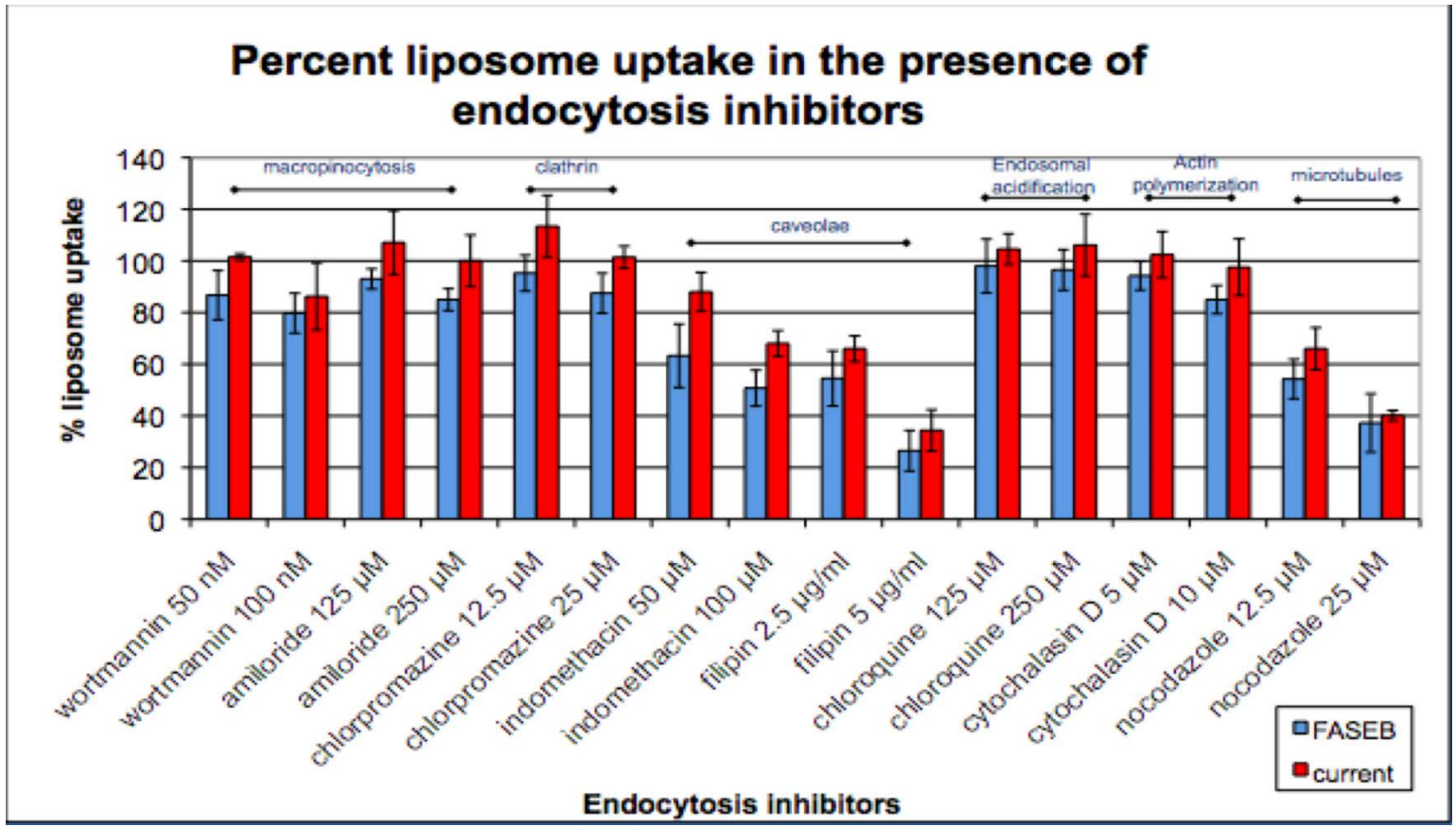


Figure 16: Comparison of uptake of rhodamine labeled monounsaturated 'ER-targeting' liposome data from this experiment (red) to the data observed for the previously published data (Pollock *et al*., 2010a) (blue), using the same formulation conditions with the same inhibitors (same concentrations/ incubation conditions) using the same endpoint analysis. N=6 for current experiment, n=3 for Pollock *et al*., 2010a data.

## 4.4 Discussion

In order to gain a better understanding as to how ER-targeting liposomes enter and traffic within cells, a comprehensive experimental design was developed and completed looking at how cellular entry and trafficking of 25 liposome formulations with varying but distinctive phospholipid compositions was affected by endocytosis and cellular trafficking inhibitors in Huh7.5 cells. Table 15 summarizes the findings from this extensive study.

**Table 15**: Summary of the cellular internalisation and trafficking mechanisms utilized by liposomes of varying phospholipid composition.

| Liposome characteristics | Cellular internalization mechanism | | | | |
|---|---|---|---|---|---|
| | Clathrin | Caveolae | Macropinocytosis | Endosomal acidification | Microtubules |
| MERLs | | ✓ | | | ✓ |
| PERLs | | ✓✓ | | | ✓ |
| PI increased | | ✓ | ✓ | | ✓ |
| PS increased | | | ✓ | | ✓ |
| pH sensitive | ✓ | | | | |

Legend: one tick indicates the higher inhibitor concentration resulted in ≥70% inhibition of liposomal uptake, two ticks indicates both inhibitor concentrations resulted in ≥70% inhibition of liposomal uptake, and no tick indicates no significant change in liposomal uptake in the prescence of the inhibitor.

Overall, the results from these experiments suggest:

- Polyunsaturated PERLs were three times more inhibited by methyl-β-cyclodextrin, a compound that sequesters cholesterol out of the plasma membrane, than monounsaturated MERLs.
- Liposomes with increased PI concentrations were inhibited by LY294002, but not Wortmannin, which inhibits phosphatidyl 3-kinase (PI3K) involved in macropinocytosis, Wortmannin inhibits PI3Kα, while LY294002 inhibits PI3Kα and β isoforms.
- Cellular uptake of liposomes with increased PS concentrations was inhibited by ethylisopropylamiloride and HOE 694, but not amiloride, which are all sodium-protein exchange inhibitors in macropinocytosis but have varying specificities.
- pH-sensitive liposomes were inhibited by chlorpromazine, which inhibits the formation of clathrin coated pits preventing clathrin-mediated endocytosis.

Previous research (Zaki & Tirelli, 2010) has shown that pH-sensitive liposomes use clathrin-mediated endocytosis that is inhibited with chlorpromazine; our data supports this. Results from the current study suggest that PI and PS both utilize macropinocytosis for cellular entry, but use different processes. The liposomes with increased PI content use a LY294002 sensitive pathway, suggesting that the inositol triphosphate (IP3) signalling pathway is involved. Interestingly, the inositol triphosphate pathway uses retrograde transport suggesting that the PI component of ER-targeting liposomes may influence their intracellular trafficking to utilize retrograde transport. PS containing liposomes use macropinocytosis for cellular entry, but appear to use a proton/sodium

exchange mechanism. It is possible that the acidic serine head group is involved in this. Although amiloride, EIPA, and HOE 694 are all macropinocytosis proton exchange inhibitors, a recent study looking at liposome cellular entry suggests that HOE694 is more potent than EIPA, which is more potent than amiloride (Koivusalo *et al.*, 2010). The fact that PERLs are three times more inhibited by methyl-β-cyclodextrin than MERLs suggests that cholesterol plays a more significant role in cellular entry for liposomes with higher unsaturation levels. Inhibiting cellular receptors and monitoring liposome uptake should further our understanding of the cellular internalisation processes involved.

It is important to consider the specificity of the inhibitors and how they may inhibit other cellular processes. When determining the maximum inhibitor concentration that can be used whilst maintaining <5% cell toxicity, the cellular morphology was also examined by light microscopy since previous publications suggest that some inhibitors do not kill the cells but severely change their morphology, especially nocodazole (Vercauteren *et al.*, 2010). Analysis by a flow cytometry, FACS, endpoint assay should produce less variable results than the spectrophotometer endpoint assay since the cell count analyzed can be normalized. This should be considered for any further experimentation in the future. Since the inhibitors used in this study may have multiple mechanisms of action and the effect on cellular behaviour is complex, adding liposomes to cell lines that are dominant-negative for a particular cellular internalisation process (such as caveolae-dependent or dynamin-dependent) could further confirm these findings. Additionally, liposomes with varying phospholipid composition could be incubated with low-density lipoprotein (LDL), high-density lipoprotein (HDL), or scavenger receptor class B type 1 (SR-B1) inhibitors to determine which phospholipids influence liposome cellular entry via these

cellular receptors. The liposomes used in this study were 50 - 300 nm in size, allowing them to utilize the many modes of cellular internalisation examined in this experiment. It would be interesting to prepare liposomes of various sizes and observe the effect on the route of cellular internalisation.

Overall, this experiment provides insight into the mechanisms of liposome cellular internalisation and the influence the phospholipid composition of a liposome has on its cellular internalisation and movement, *in vitro*. Liposomes containing phosphatidylinositol, PI, and phosphatidylserine, PS, utilize macropinocytosis for cellular internalisation but have different mechanisms to do so. Developing liposomal formulations that avoid clathrin endocytosis and endosomal acidification will allow the liposomes to have increased stability within the cell, giving more efficient and potentially specific cargo delivery within the cell. Understanding how the phospholipid composition influences cellular internalisation and trafficking processes is crucial to understanding how liposome cargos, such as drugs, are delivered and utilized within the cell. These experimental findings add to the knowledge of liposomal endocytosis and cellular trafficking and will hopefully be built upon in the future.

# Chapter five: Conclusions

In order to further the understanding of how 'ER-targeting' liposomes may encapsulate small molecules of varying chemical properties, this research used two types of iminosugars, known α–glucosidase inhibitors, with different hydrophobic and polar attributes to dissect what effect these properties have on the molecule's ability to become encapsulated by liposomes. The model small molecule iminosugars with varying chemical properties to be encapsulated in 'ER-targeting' liposomes were *N*B-DNJ, a hydrophilic molecule and NAP-DNJ, a hydrophobic molecule.

In order to determine quantitatively the encapsulation efficiency of these iminosugars, robust and quantitative analytical methods needed to be developed. Although this may sound trivial at the onset, due to the extreme differences in the chromatographic properties of liposomes and iminosugars and the lack of a chromophore in the iminosugar *N*B-DNJ, this was quite a challenging analytical endeavor. Without a chromophore to aid ultraviolet detection, the analytical detection possibilities were quite limited. Originally it was hoped that ionic properties could be exploited using cation exchange chromatography paired with pulsed amperometric detection, since this combination had successfully been used previously to detect *N*B-DNJ (Mellor *et al.*, 2000). However, after extensive efforts to optimize the sample purification to remove lipids and liposomes, the separation of the cation exchange chromatography, and the electrochemical detection parameters of the pulsed amperometric detection system this research determined that the

cation exchange chromatography paired with pulsed amperometric detection could not robustly analyze samples containing liposomes, due to the liposomes and lipids fouling the gold electrode in the electrochemical detector. The alternate detection methods that could be used to detect compounds without chromophores were refractive index detection, evaporative light scattering detection, and mass spectrometric detection. Refractive index detection paired with reverse phase chromatography was chosen since it was readily accessible and presents an economic approach. One of the main limitations of developing analytical methods on refractive index chromatographic systems is that they may only use isocratic chromatographic methods since gradient chromatographic methods that vary the solvent composition throughout the analysis are not compatible with refractive index detection. The encapsulation efficiency of *N*B-DNJ was determined using a method developed using reverse phase chromatography paired with refractive index detection (RP-RID). However, the peak resolution between the 'ER-targeting' liposomes and the *N*B-DNJ chromatographic peaks could certainly be improved. Several attempts were tried to improve these peaks' resolution but the challenge proved difficult since gradient chromatographic methods could not be employed. Several solvents were tried as the sample diluent and/ or mobile phase without increasing the peak resolution. Cation exchange chromatography paired with refractive index detection was explored without success due to further coeluting peaks. Normal phase chromatography paired with refractive index chromatography resulted without *N*B-DNJ retention on the analytical column. Several column pairings were attempted to detect both the liposomes and *N*B-DNJ analyte with improved peak resolution without any further success. Many attempts were made to remove the lipids and liposomes from the sample matrix in order to analyze the *N*B-DNJ analyte alone; however, none of the sample preparation methods

attempted were able to entirely remove the liposomes/lipids. Any lipid or liposome coeluting with the *N*B-DNJ leads to an unreliable quantitative method. The reverse phase chromatography refractive index method used to determine the encapsulation efficiency of *N*B-DNJ in 'ER-targeting' liposomes had enough peak resolution for proper integration of individual peaks at 1 mM concentrations, but the integration of the peaks became difficult at higher concentrations. The next step of tackling this coelution issue would be to develop LC/MS methods that could quantitatively determine how much of the *N*B-DNJ analyte is in the coeluted peak. The instrumentation involved in developing this method was not readily available at the time of this research, but would be highly recommended for future studies.

There were no known quantitative analytical methods for detecting NAP-DNJ prior to this research. However, since NAP-DNJ had a chromophore UV detection could be used, making the analytical method development much more traditional and straightforward than the *N*B-DNJ analytical method development. A robust quantitative reverse phase gradient chromatography method paired with UV detection was developed for NAP-DNJ and then applied to analyze encapsulated NAP-DNJ in 'ER-targeting' liposome samples. Since the UV detection allows the chromatographic gradient's properties to be exploited, there were no issues with liposome and NAP-DNJ peak coelution. The encapsulation efficiencies of several concentrations of NAP-DNJ in 'ER-targeting' liposomes were determined using this RP-UV method. The main challenge with determining the encapsulation efficiency of NAP-DNJ in liposomes was that NAP-DNJ is hydrophobic, hence difficult to dissolve and formulate in the primarily aqueous liposome formulation conditions. A colleague, Kong Tang, optimized the formulation procedure for NAP-DNJ

‘ER-targeting’ liposomes and determined the maximum loading concentration of NAP-DNJ to be 2 mM (Tang, 2012). This was one of the many differences observed of how the different properties of the iminosugars affected their ability to be encapsulated into liposomes.

The most profound difference observed for the different iminosugars’ ability to be encapsulated into liposomes were their hydrophobic and hydrophilic properties. The hydrophilic nature of *N*B-DNJ allowed it to be encapsulated in pH-sensitive and ‘ER-targeting’ liposome formulations in a linear trend up to 80 mM. The hydrophobic nature of NAP-DNJ seemed to influence the molecule’s ability to become encapsulated in ‘ER-targeting’ liposomes, with the highest concentration to become robustly incorporated being 2 mM. Both *N*B-DNJ and NAP-DNJ had similar encapsulation efficiencies of approximately 5% at 1 mM concentration in 5 mM ‘ER-targeting’ liposomal formulations. However, the ability of *N*B-DNJ to become encapsulated in liposomes increased proportionally with an increase in loading concentration of *N*B-DNJ, whereas the ability of NAP-DNJ to be encapsulated in liposomes was inversely proportional to concentration of NAP-DNJ, meaning that higher encapsulation efficiencies were obtained for formulations with lower NAP-DNJ concentrations. This is likely due to the differences in hydrophobicity between the two iminosugars. Since the phospholipids that comprise a liposome have both polar and non-polar regions - the head group being primarily polar and the acyl side chains of various lengths being primarily non-polar - both polar and non-polar molecules may interact with the phospholipids in different manners and both may become incorporated into phospholipids and liposomes. This research concludes that the hydrophobicity of a small molecule plays a much larger role

in its ability to become incorporated or encapsulated into a liposomal formulation than its polarity.

Hopefully the information gained through this research will aid future researchers with knowledge and new considerations when formulating iminosugars as drug therapies in liposomal drug delivery vesicles. The iminosugar concentration that yields the highest encapsulation efficiency is considerably different for each iminosugar and should be taken into account when designing the dose ranges of future preclinical and clinical trials. The liposome formulation technique used in this research was a commonly used technique known as reverse-phase phase evaporation. There are many methods for liposomal formulation that could be considered to improve the encapsulation efficiency and increase the amount of drug delivered by the liposomes (Riaz, 1996). The quantitative analytical methods developed here should be helpful for any future studies analyzing iminosugars delivered by liposomes.

The next question this research hoped to answer was what influence does the phospholipid composition of a liposome have on its *in vitro* cellular internalization and trafficking processes? In order to probe the answer to this question, an extension study was completed using many fluorescently labeled liposome formulations with distinct phospholipid characteristics. These liposomes were added *in vitro* to cells with known cellular internalization and trafficking inhibitors. The hope behind generating this information was to gain a better understanding of how each phospholipid affects the cellular internalization mechanisms that a liposome is subject to, and its subsequent movement within the cell. This information could be used to develop more specific and

directly targeting liposomes, potentially lowering the concentrations of cargo to be delivered by the liposomes. One of the main endocytosis pathways of interest to try to circumvent is the clathrin mediated endocytosis pathway. This is generally thought to lead to endosomal acidification, which results in lysis in the lysosome or degradation along the endosomal pathway (Doherty & McMahon, 2009). The idea is that by using more specific intracellular delivery with liposomes, lower concentrations of drugs may be delivered to achieve the same clinical effect. This would potentially open avenues for effective delivery of drugs that may previously have had toxicity issues due to the large concentrations required when dosed without liposomal or organelle-targeting liposomal delivery. This research observed the effect of cellular endocytosis and trafficking inhibitors on the uptake of fluorescently labeled liposomes of varying phospholipid compositions into cells. The study used pH-dependent liposomes, monounsaturated 'ER-targeting' liposomes, and polyunsaturated 'ER-targeting' liposomes formulations. Since phosphatidylinositol and phosphatidylserine had been previously determined crucial for ER-targeting the concentrations of these were intensified to see the effect of cellular internalization and trafficking mechanisms. The liposomes' stability was determined by stable particle size determined by dynamic light scattering analysis.

The overall conclusions of the study were that the polyunsaturated 'ER-targeting' liposomes were inhibited three times as much by methyl-β-cyclodextrin than monounsaturated 'ER-targeting' liposomes were. One of the main things that methyl-β-cyclodextrin is known to do is to sequester cholesterol out of the plasma membrane. The results from this study suggest that increased unsaturation in liposome formulations may require more involvement or interaction with cholesterol for cellular entry *in vitro*. The

liposomes with higher concentrations of PI and PS were both affected by macropinocytosis inhibitors suggesting that they both utilize macropinocytosis as a cellular internalisation mechanism. However, the liposome formulations with increased phosphatidylinositol concentrations were affected by an inhibitor of PI3Kβ process involved in macropinocytosis membrane ruffling, LY294002. The liposome formulations with increased phosphatidylserine concentrations were affected by a sodium protein exchange inhibitor involved in macropinocytosis membrane ruffling, ethylisopropylamiloride (EIPA) and HOE 694. These results show that although the PI and PS phospholipids both utilize macropinocytosis for cellular internalisation *in vitro*, they do so via different mechanisms. The pH-sensitive liposomes were affected by inhibitors of clathrin-mediated endocytosis, and the 'ER-targeting' liposomes were affected by inhibitors of caveolae mediated endocytosis. This aligns with previous research (Simões, 2001; Pollock, 2010a).

Isolating the mechanisms involved with cellular internalisation and trafficking mechanisms is difficult for many reasons, but one of the challenges of this study was that most inhibitors of these cellular processes are complex, not fully understood, and/or have known multiple effects on cellular processes. In order to further the knowledge gained by this research, dominant negative mutant cell lines of the individual cellular inhibitors (ex. dynamin dominant negative HepaRG cell line) could be used to see more of the whole picture of the liposomes interacting with a particular cellular internalisation or movement process. This research looked at the cellular internalisation and endocytosis processes involved in liposomal cellular entry, but did not explore the cellular receptors that are likely to be involved. Future studies might want to explore how the LDL, HDL, acLDL,

and SR-B1 cell surface receptors are involved with liposomal entry of liposomes made of varying phospholipid compositions.

This research furthered the understanding of the influence that phospholipid composition has on cellular entry and movement, however it is a complex environment from which it is difficult to isolate exact and certain causal effects of phospholipids on cellular processes. This information was a useful screening exercise to isolate the key cellular uptake inhibitors and phospholipid properties that liposomes use that could aid liposomal drug delivery research. Liposomal drug delivery shows promise for expanding the possibilities for delivering drugs more efficiently and this research has expanded the knowledge of liposomal delivery of iminosugars that will hopefully be useful for future clinical research.

# Appendices

## Appendix A: Chemical structures

### A1: Calcein

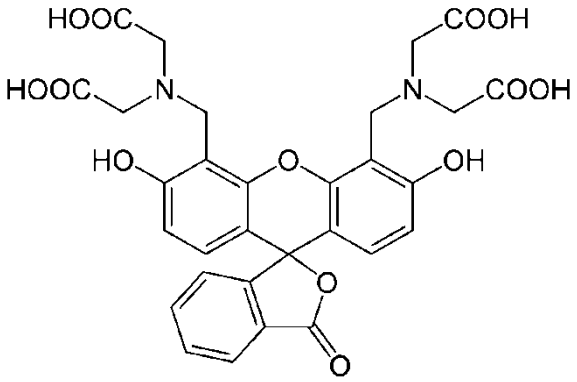


### A2: Glucose and iminosugars

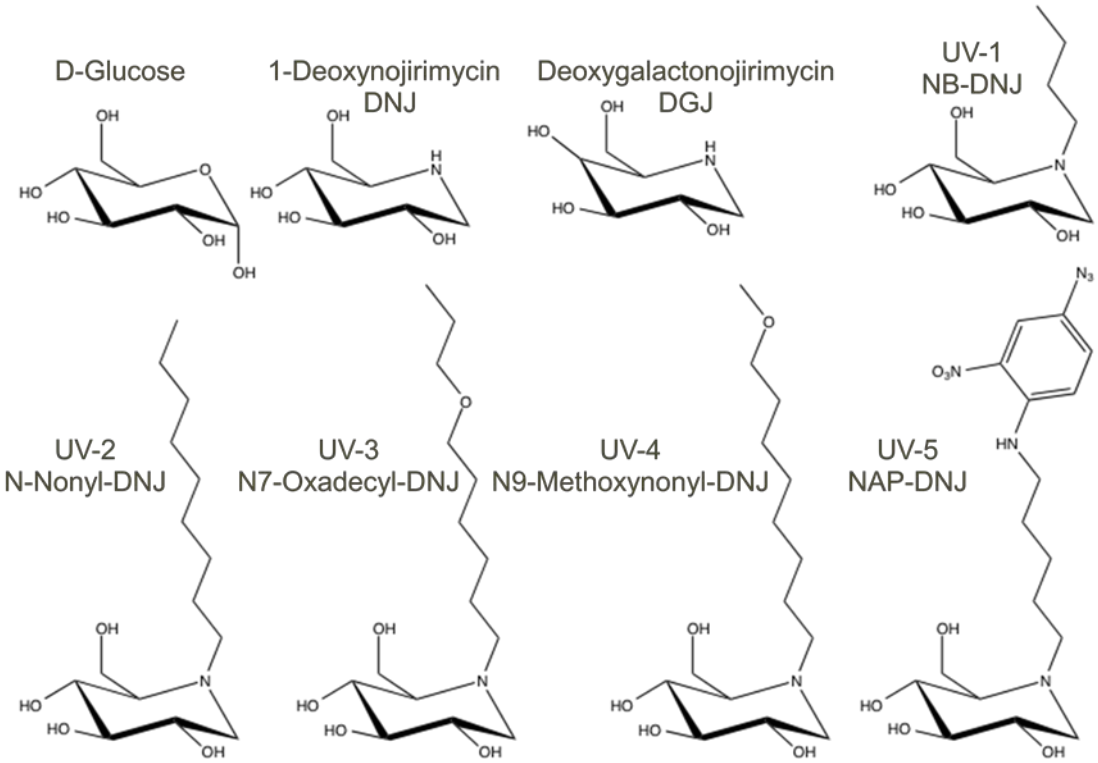

## A3: Phospholipids

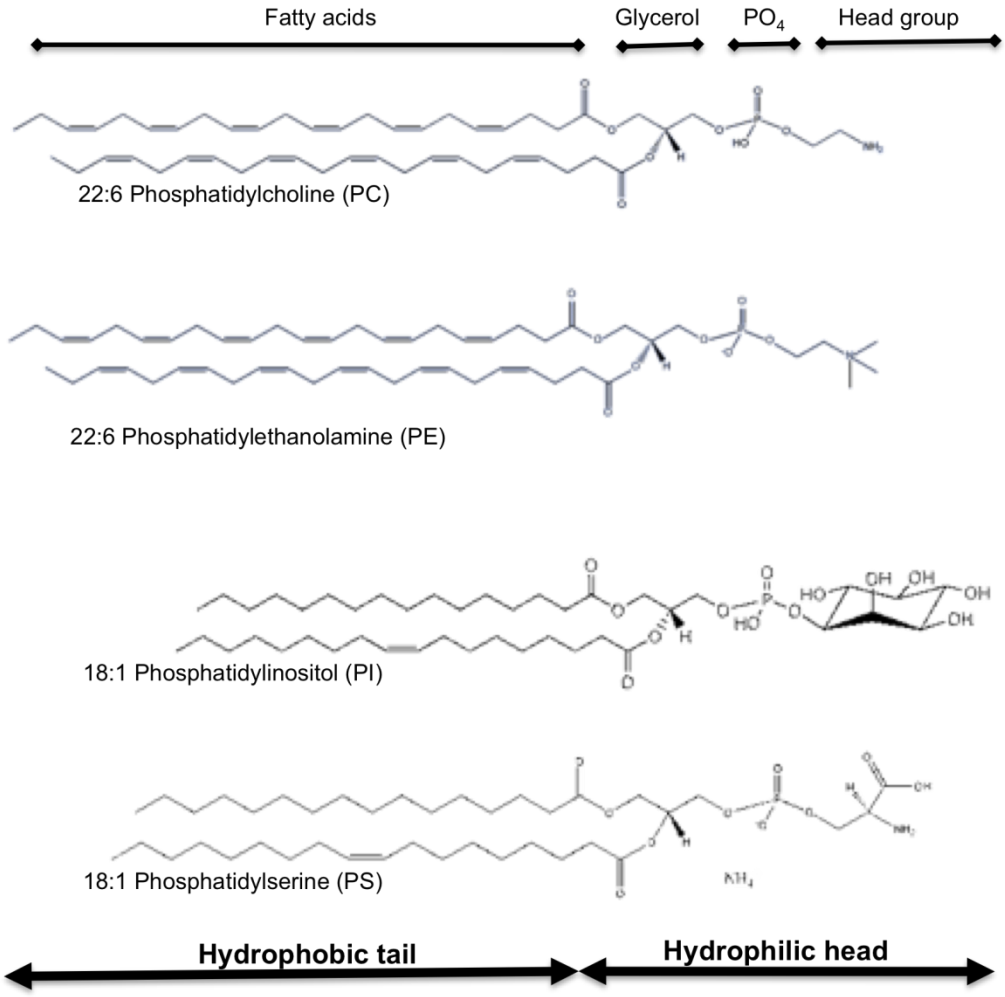

NBD-PE, 1,2-dioleoyl-*sn*-glycero-3-phosphoethanolamine-

N-(7-nitro-2-1,3-benzoxadiazol-4-yl) (ammonium salt):

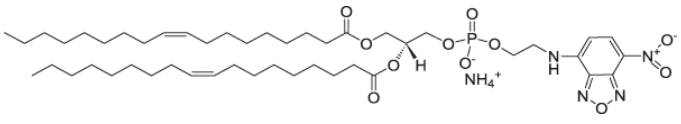

Lissamine rhodamine B-PE, 1,2-dioleoyl-*sn*-glycero-3-phosphoethanolamine-

N-(lissamine rhodamine B sulfonyl) (ammonium salt):

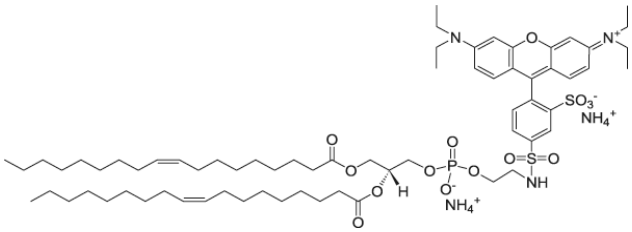

DOPE, 1,2-dioleoyl-*sn*-glycero-3-phosphoethanolamine:

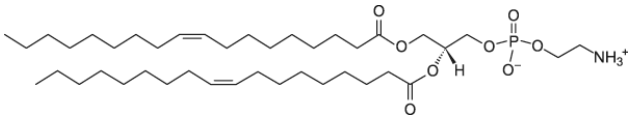

DOPC, 1,2-dioleoyl-*sn*-glycero-3-phosphocholine:

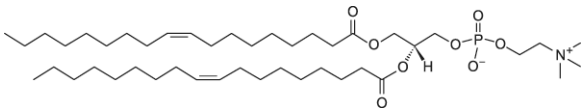

PI, L-α-phosphatidylinositol (Liver, Bovine) (sodium salt) :

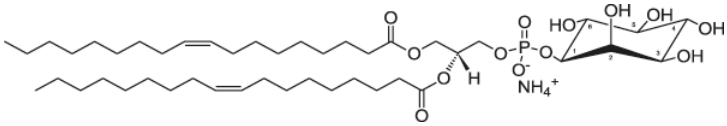

PS, L-α-phosphatidylserine (Brain, Porcine) (sodium salt):

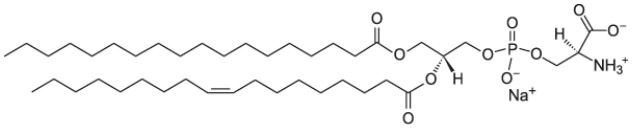

**A4: Sterols**

CHEMS, cholesterol hemisuccinate:

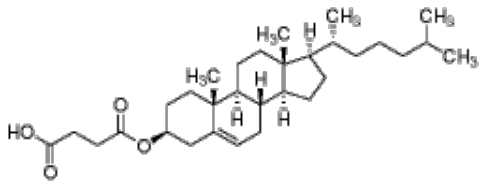


Tocopherol:

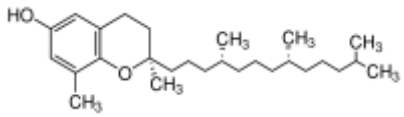

# Appendix B: Materials

| Name of the reagent | Company | Catalogue # | Comments |
|---|---|---|---|
| 18:1 Lissamine rhodamine B- PE | Avanti | 810150C | Headgroup labeled, 1 mg |
| DOPE | Avanti | 850725C | 25 mg |
| 22:6 PE | Avanti | 850797C | 25 mg |
| DOPC | Avanti | 850375C | 25 mg |
| 22:6 PC | Avanti | 850400C | 25 mg |
| PI, natural | Avanti | 840042C | 25 mg |
| 18:1 PI | Avanti | 850149C | 100 μg |
| PS, natural | Avanti | 840032C | 25 mg |
| 18:1 PS | Avanti | 840035C | 25 mg |
| CHEMS | Sigma | C-6512 | |
| Tocopherol | Sigma | T3251 | |
| Chlorpromazine | Sigma | C8138 | |
| Indomethacin | Sigma | I7378 | |
| Chloroquine | Sigma | C6628 | |
| Cytochalasin D | Sigma | C8273 | |
| Metyl-beta-cyclodextran | Sigma | C4555 | |
| Filipin | Sigma | F4767 | |
| Bafilomycin A | Sigma | B1793 | |
| HOE 694 | - | - | gift from Robert Wilkins |
| LY 294002 | Sigma | L9908 | |
| Nocodazole | Sigma | M1404 | |
| Nystatin | Sigma | N6261 | |
| Wortmannin | Sigma | W1628 | |
| TES | Sigma | 2-[[1,3-dihydroxy-2-(hydroxymethyl)propan-2-yl]amino]ethanesulfonic acid, T5691 | |

| Name of the reagent | Company | Catalogue # | Comments |
|---|---|---|---|
| Amiloride | Sigma | A7410 | |
| EIPA | Sigma | A3085 | |
| Dynasore | Sigma | D7693 | |
| Genistein | Sigma | G6649 | |
| IonPack CS10 column | Dionex | 043015 | 4 x 250 mm |
| CSRS 300 micromembrane supressor | Dionex | 064556 | 4 mm |
| Zorbax C18 column | Agilent | 7995118-595 | 5 μm, 4.6 x 150 mm |
| 1.8 ml HPLC vials | Waters | 186000273 | 12 x 32 screw top |
| 1.8 ml HPLC vial caps | Waters | 1521503130 | PTFE silicone septa |
| Mini extruder | Avanti | 610023 | 1ml syringes |
| Filter supports | Avanti | 610014 | |
| 0.1 μM filter membrane | Whatman | 800309 | PCMB |
| Syringe filter | Nalgene | 180-1320 | 0.22 μM, PES |
| Sephadex G-50 medium | GE Healthcare | 17-0043-01 | |
| PD-10 columns | GE Healthcare | 17-0851-01 | Sephadex G-25 |
| Fetal bovine serum | Gibco | 10270-106 | |
| DMEM w/o phenol red | Invitrogen | 31053-028 | |
| Trypsin-EDTA | Sigma | T3924 | |
| Penicillin-Streptomycin | Sigma | P0781 | |
| L-glutamine | Sigma | G7513 | |
| 1x DPBS | PAA | HIS-002 | No Ca2+ / Mg2+ |
| PBS | Sigma | D8537 | |
| *N*B-DNJ | United Therapeutics | D-1032-064 | UV-1 |
| NAP-DNJ | United Therapeutics | 14108-PH14b2 | UV-5 |
| Calcein | Sigma | C0875-10G | |

| Name of the reagent | Company | Catalogue # | Comments |
|---|---|---|---|
| CellTiter 96 $AQ_{ueous}$ One Solution | Promega | TB245 | MTS Assay |
| sodium chloride | Sigma | S-3014 | |
| Triton X-100 | Fischer | T/3751/08 | |
| 2-morpholinoethansulfonic acid | Fischer | BPE300-100 | |
| Acetonitrile | Rathburn | RH1016 | HPLC grade |
| Trifluoroacetic acid | Rathburn | PTS6045 | HPLC grade |
| 26.5 M Formic acid | Romil-SpS | H353 | |
| 50% sulfuric acid | Fluka | 84733 | puriss grade |
| Solid phase extraction tube | Interchrom | 97730 | |
| Strong cation exchange column | Varian | 12102013 | BondElut |
| C18 reverse phase cartridge column | Waters | WAT023590 | |
| Huh7.5 cells | Apath LLC | St. Louis, MO | |
| DAPI Vectorshield | Vector Labratories, | Burlingame, CA | |

# Appendix C: Protocols

**Protocol for preparing liposomes using reverse phase hydration**

1. Remove lipid stocks from freezer and allow time for them to equilibrate to ambient conditions.
2. Add appropriate amount of the combination of lipids desired to a glass vial, under Nitrogen. Ensure the lipids stock vials are kept minimally open to prevent/ reduce oxidation. Add Nitrogen to the lipid stock vials and the formulation vial(s) to reduce oxidation.
3. After all the lipids are added to the formulation vial, vortex briefly to mix the lipids thoroughly.
4. Dry the lipid mixture under a gentle Nitrogen gas stream while rotating the vial to prevent agglomeration. Once the lipid mixture is dry it will appear as a film on the bottom of the formulation vial.
5. Add an appropriate amount of the resuspension diluent, such as PBS or drug solution to ensure the final desired concentration is achieved, ie 5 mM or 10 mM.
6. Vortex formulation vial for 2-4 hours at a temperature above the phase transition temperature of the liposome formulation. Vortex until lipid film is completely resuspended.
7. While the formulation is being vortexed, prepare the mini-extruder by cleaning all of its components in sterile water then ethanol and soak the filter supports and membrane(s) in PBS for five minutes.

8. Prepare the mini-extruder apparatus by placing a filter support disk on each barrel within the O-ring and a membrane on top of one barrel/support disk making sure no air bubbles are present. Assemble the mini-extruder apparatus and screw together tightly.
9. Fill one syringe with the diluent and attach to the apparatus. Attach the remaining, empty syringe to the apparatus. Pass the diluent through the mini-extruder a couple of times to ensure that the apparatus is assembled correctly and without leaks. Pass the diluent entirely into one syringe, then remove that syringe and discard the diluent.
10. Add at least 300 µL of the liposome formulation to the syringe and attach to the mini-extruder apparatus. Adding less than 300 µL may result in insufficient volume to pass through the membrane assembly robustly and could produce highly variable liposome particle sizes.


11. Pass the liposome formulation through the membrane at least 11 times or more, ensuring that it is an odd number of times so that when the syringe in finally removed it will contain the liposome formulation of the intended particle size.

This process should be done above the phase transition temperature of the liposome formulation and a heat block apparatus may be required.


12. The liposome formulation should now be at a uniform particle size. The particle size distribution should now be determined by dynamic light scattering (DLS).
13. Store liposome formulations at 4 °C. Mini-extruder apparatus should be cleaned throroughly with sterile water and dried with ethanol before storage.

# References

ARCARO, A. and WYMANN, M.P., 1993. Wortmannin is a potent phosphatidylinositol 3-kinase inhibitor: the role of phosphatidylinositol 3,4,5-trisphosphate in neutrophil responses. *Biochem. J.*, **296**(2), pp. 297-301.

BLOCK, T.M., LU, X., PLATT, F.M., FOSTER, G.R., GERLICH, W.H., BLUMBERG, B.S. and DWEK, R.A., 1994. Secretion of human hepatitis B virus is inhibited by the imino sugar N- butyldeoxynojirimycin. *PNAS*, **91**, pp. 2235-2239.

BRENNAN, T.M., TAYLOR, D.L., BRIDGES, C.G., LEYDA, J.P. and TYMS, A.S., 1995. The inhibition of human immunodeficiency virus type 1 in vitro by a nonnucleoside reverse transcriptase inhibitor MKC-442, alone and in combination with other anti-HIV compounds. *Antiviral Res.*, **26**, pp. 173-187.

CHAPEL, C., GARCIA, C., BARTOSCH, B., ROINGEARD, P., ZITZMANN, N., COSSET, F. DUBUISSON, J., DWEK, R.A., TRÉPO, C., ZOULIM, F., and DURANTEL, D., 2007. Reduction of the infectivity of hepatitis C virus pseudoparticles by incorporation of misfolded glycoproteins induced by glucosidase inhibitors. *Journal of Gen. Virol.*, **88**, pp. 1133-1143.

COMPAIN, P., MARTIN, O.R., BOUCHERON, C., GODIN, G., IKEDA, K., and ASONA, N., 2006. Design and synthesis of highly potent and selective pharmaceutical chaperones for the treatment of Gaucher's disease. *Chembiochem.,* **7**(9), pp 1356-1359.

CORVERA, S. and CZECH, M.P., 1998. Direct targets of phosphoinositide 3-kinase products in membrane traffic and signal transduction. *Trends in Cell Biol.,* **8**(11), pp. 442-446.

COSTIN, G., TRIF, M., NICHITA, N., DWEK, R.A. and PETRESCU, S.M., 2002. pH-sensitive liposomes are efficient carriers for endoplasmic reticulum-targeted drugs in mouse melanoma cells. *Biochem Biophys Res Commun.,* **293**, pp. 918-923.

DIJKSTRA, J., VAN GALEN, M. and SCHERPHOF, G.L., 1984. Effects of ammonium chloride and chloroquine on endocytic uptake of liposomes by Kupffer cells in vitro. *Biochim Biophys Acta.,* **804**(1), pp. 58-67.

DIONEX CORPORATION, 2000. *Analysis of Carbohydrates by High Performance Anion Exchange Chromatography with Pulsed Amperometric Detection (HPAE-PAD).* Technical Note 20. Sunnyvale, CA: Dionex Corporation.

DOHERTY, G.J. and MCMAHON, H.T., 2009. Mechanisms of Endocytosis. *Annu Rev Biochem.,* **78**, pp. 857-902.

ELSTEIN, D., HOLLAK, C., AERTS, J. M., VAN WEELY, S., MAAS, M., COX, T.M., LACHMANN, R.H., HREBICEK, M., PLATT, F.M., BUTTERS, T.D., DWEK, R.A. and ZIMRAN, A., 2004, Sustained therapeutic effects of oral miglustat (Zavesca, N-butyldeoxynojirimycin, OGT 918) in type I Gaucher disease. *J Inherit Metab Dis.*, **27**(6), pp. 757-766.

FISCHER, P.B., COLLIN, M., KARLSSON, G.B., JAMES, W., BUTTERS, T.D., DAVIS, S.J., GORDON, S., DWEK, R.A., and PLATT, F.M., 1995. The alpha-glucosidase inhibitor N-butyldeoxynojirimycin inhibits human immunodeficiency virus entry at the level of post-CD4 binding. *Journal Virol.*, **69**, pp. 5791-5797.

FISCHL, M., RESNICK, L., COOMBS, R., KREMER, A., POTTAGE, J.J., FASS, R., FIFE, K.H, POWDERLY, W.G., COLLIER, A.C., and ASPINALL, R.L., and *ET AL*., 1994. The safety and efficacy of combination N-butyl-deoxynojirimycin (SC-48334) and zidovudine in patients with HIV-1 infection and 200–500 CD4 cells/mm3. *J Acquir Immune Defic Syndr.,* **7**, pp. 139-147.

GÖTTE, M., SOFEU FEUGAING, D.D. and KRESSE, H., 2004. Biglycan is internalized via a chlorpromazine-sensitive route. *Cell. Mol. Biol. Lett,* **9**(3), pp. 475-481.

HAYER, A., STOEBER, M., BISSIG, C. and HELENIUS, A., 2010. Biogenesis of caveolae: stepwise assembly of large caveolin and cavin complexes. *Traffic,* **11**(3), pp. 361-382.

HILLAIREAU, H. and COUVREUR, P., 2009. Nanocarriers' entry into the cell: relevance to drug delivery. *Cell Mol Life Sci.,* **66**(2873), pp. 2896-2009.

HUTH, U.S., SCHUBERT, R. and PESCHKA-SÜSS, R., 2006. Investigating the uptake and intracellular fate of pH-sensitive liposomes by flow cytometry and spectral bio-imaging. *Journal of Controlled Release*, **110**, pp. 490-504.

ISSA, M.M., KÖPING-HÖGGÅRD, M., TØMMERAAS, K., VÅRUM, K.M., CHRISTENSEN, B.E., STRAND, S.P. and ARTURSSON, P., 2006. Targeted gene delivery with trisaccharide-substituted chitosan oligomers in vitro and after lung administration in vivo. *J Control Release.,* **115**(1), pp. 103-112.

JORDAN, R., NIKOLAEVA, O.V., WANG, L., CONYERS, B., MEHTA, A., DWEK, R.A. and BLOCK, T.M., 2002. Inhibition of host ER glucosidase activity prevents golgi processing of virion-associated bovine viral diarrhea virus E2 glycoproteins and reduces infectivity of secreted virions. *Virology,* **295**, pp. 10-19.

KOIVUSALO, M., WELCH, C., HAYASHI, H., SCOTT, C.C., KIM, M., ALEXANDER, T., TOURET, N., HAHN, K.M. and GRINSTEIN, S., 2010. Amiloride inhibits macropinocytosis by lowering submembranous pH and preventing Rac1 and Cdc42 signaling. *J Cell Biol.,* **188**(4), pp. 547-563.

MACIA, E., EHRLRICH, M., MASSOI, R., BOUCROT, E., BRUNNER, C., KIRCHHAUSEN, T., 2006. Dynasore: A cell-permeable inhibitor of Dynamin. *Dev. Cell.,* **10** (1), pp 839-850.

MANUNTA, M., NICHOLS, B.J., TAN, P.H., SAGOO, P., HARPER, J. and GEORGE, A.J., 2006. Gene delivery by dendrimers operates via different pathways in different cells, but is enhanced by the presence of caveolin. *J Immunol Methods,* **314**(1-2), pp. 134-146.

MELLOR, H.R., ADAM, A., PLATT, F.M., DWEK, R.A. and BUTTERS, T.D., 2000. High-performance cation-exchange chromatography and pulsed amperometric detection for the separation, detection, and quantitation of N-alkylated imino sugars in biological samples. *Anal Biochem.,* **284**(1), pp. 136-142.

MELLOR, H.R., NEVILLE, D.C., HARVEY, D.J., PLATT, F.M., DWEK, R.A. and BUTTERS, T.D., 2004. Cellular effects of deoxynojirimycin analogues: inhibition of N-linked oligosaccharide processing and generation of free glucosylated oligosaccharides. *Biochem J.,* **381**(3), pp. 867-875.

PARTON, R.G., 2004. Caveolae meet endosomes: a stable relationship? *Dev Cell.,* **7**(4), pp. 458-460.

PAULSEN, H. and BROCKHAUSEN, I., 2001. From imino sugars to cancer glycoproteins. *Glycoconj J.,* **18**(11-12), pp. 867-870.

POLLOCK, S., DWEK, R.A., BURTON, D.R. and ZITZMANN, N., 2008a. N-Butyldeoxynojirimycin is a broadly effective anti-HIV therapy significantly enhanced by targeted liposome delivery. *AIDS*, **22**(15), pp. 1961-1969.

POLLOCK, S., 2008b. *Liposome-based antiviral therapies.*, University of Oxford.

POLLOCK, S., ANTROBUS, R., NEWTON, L., KAMPA, B., ROSSA, J., LATHAM, S., NICHITA, N.B., DWEK, R.A. and ZITZMANN, N., 2010a. Uptake and trafficking of liposomes to the endoplasmic reticulum. *FASEB*, **24**, pp. 1866-1878.

POLLOCK, S., NICHITA, N.B., BÖHMER, A., RADULESCU, C., DWEK, R.A. and ZITZMANN, N., 2010b. Polyunsaturated liposomes are antiviral against hepatitis B and C viruses and HIV by decreasing cholesterol levels in infected cells. *PNAS*, **107**(40), pp. 17176-17181.

RIAZ, M., 1996, Liposomes preparation methods. *Pak J Pharm Sci.*, **19**(1), pp. 65-77

QADDOUMI, M.G., UEDA, H., YANG, J., DAVDA, J., LABHASETWAR, V. and LEE, V.H., 2004. The characteristics and mechanisms of uptake of PLGA nanoparticles in rabbit conjunctival epithelial cell layers. *Pharm. Res.*, **21**(4), pp. 641-648.

RATNER, L. and VANDER HEYDEN, N., 1993. Mechanism of action of N-butyl deoxynojirimycin in inhibiting HIV-1 infection and activity in combination with nucleoside analogs. *AIDS Res Hum Retroviruses.*, **9**, pp. 291-297.

SIMÕES, S., SLEPUSHKIN, V., DÜZGÜNES, N. and PEDROSO DE LIMA, M.C., 2001. On the mechanisms of internalization and intracellular delivery mediated by pH-sensitive liposomes. *Biochim Biophys Acta.*, **1515**, pp. 23-27.

SOLDATI, T. and SCHLIWA, M., 2006. Powering membrane traffic in endocytosis and recycling. *Nat Rev Mol Cell Biol.*, **7**(12), pp. 897-908.

STEINMANN, E., WHITFIELD, T., KALLIS, S., DWEK, R.A., ZITZMANN, N., PIETSCHMANN, T. and BARTENSCHLAGER, R., 2007. Antiviral effects of amantadine and iminosugar derivatives against hepatitis C virus. *Hepatology,* **46**, pp. 330-338.

SUN, X., LI, F., WANG, Y. and LIANG, W., 2010. Cellular uptake and elimination of lipophilic drug delivered by nanocarriers, *Pharmazie*, **65**, pp. 737-742.

SWIFT, L.L., 1995. Assembly of very low density lipoproteins in rat liver: a study of nascent particles recovered from the rough endoplasmic reticulum. *J Lipid Res.*, **35**(3), pp. 395-406.

TANAKA, Y., KATO, J., KOHARA, M. and GALINSKI, M.S., 2006. Antiviral effects of glycosylation and glucose trimming inhibitors on human para-influenza virus type 3. *Antiviral Res.*, **72**, pp. 1-9.

TANG, K., 2012. *In vitro evaluation of liposome encapsulated iminosugars as antiviral treatment against HCV*, University of Oxford.

THOMSEN, P., ROEPSTORFF, K., STAHLHUT, M. and VAN DEURS, B., 2002. Caveolae are highly immobile plasma membrane microdomains, which are not involved in constitutive endocytic trafficking. *Mol Biol Cell.*, **13**(1), pp. 238-250.

TIERNEY, M., POTTAGE, J., KESSLER, H., FISCHL, M., RICHMAN, D., MERIGAN, T. POWDERLY, W., SMITH, S., KARIM, A., SHERMAN, J., and *ET AL.* ,1995. The tolerability and pharmacokinetics of N-butyl- deoxynojirimycin in patients with advanced HIV disease (ACTG 100). The AIDS Clinical Trials Group (ACTG) of the National Institute of Allergy and Infectious Diseases. *J Acquir Immune Defic Syndr.*, **10**, pp. 549-553.

TORCHILIN, V.P., 2005. Recent advances with liposomes as pharmaceutical carriers. *Nat Rev Drug Discov.*, **4**, pp. 145-160.

VERCAUTEREN, D., VANDENBROUCKE, R.E., JONES, A.T., REJMAN, J., DEMEESTER, J., DE SMEDT, S.C., SANDERS, N.N. and BRAECKMANS, K.,

2010. The use of inhibitors to study endocytic pathways of gene carriers: optimization and pitfalls. *Mol Ther*. **18**(3), pp. 561-569.

WU, S.F., LEE, C.J., LIAO, C.L., DWEK, R.A., ZITZMANN, N. and LIN, Y.L., 2002. Antiviral effects of an iminosugar derivative on flavivirus infections., *J Virol*., **76**, pp. 3596-3604.

YUMOTO, R., NISHIKAWA, H., OKAMOTO, M., KATAYAMA, H., NAGAI, J. and TAKANO, M., 2006. Clathrin-mediated endocytosis of FITC-albumin in alveolar type II epithelial cell line RLE-6TN. *Am J Physiol Lung Cell Mol Physiol*., **290**(5), pp. 946-955.

ZAKI, N. and TIRELLI, N., 2010. Gateways for the intracellular access of nanocarriers: a review of receptor-mediated endocytosis mechanisms and of strategies in receptor targeting. *Expert Opin Drug Deliv.*, **7**(8), pp. 895-913.